

Table 2. Association of expression of the actinin-4 variant with clinicopathological characteristics of high-grade neuroendocrine tumour (HGNT) patients

Characteristic	Actinin-4 splice variant			P value ^a
	Total	Positive (%)	Negative (%)	
Sex				
Male	143	78 (55%)	65 (46%)	1
Female	33	18 (55%)	15 (46%)	
Age				
≥65 years	105	60 (57%)	45 (43%)	0.442
<65 years	71	36 (51%)	35 (49%)	
Smoking status				
Never smoked	7	3 (43%)	4 (57%)	0.703
Current or former smoker	169	93 (55%)	76 (45%)	
Histological subtype				
SCLC	70	42 (60%)	28 (40%)	0.280
LCNEC	106	54 (51%)	52 (49%)	
Pathological stage ^b				
I, II	124	62 (50%)	62 (50%)	0.069
III, IV	52	34 (65%)	18 (35%)	
Tumour size				
≤3 cm	94	56 (60%)	38 (40%)	0.173
>3 cm	82	40 (49%)	42 (51%)	
Lymph node metastasis				
Absent	101	50 (50%)	51 (51%)	0.129
Present	75	46 (61%)	29 (39%)	
Distant metastasis				
Absent	170	92 (54%)	78 (46%)	0.690
Present	6	4 (67%)	2 (33%)	
Recurrence				
Absent	91	39 (43%)	52 (57%)	0.00200
Present	79	53 (67%)	26 (33%)	

SCLC, small cell lung carcinoma; LCNEC, large cell neuroendocrine carcinoma.

^aFisher's exact test. P values of <0.05 are shown in bold.

^bAccording to the International Union Against Cancer (UICC) TNM Classification of Malignant Tumours, 7th edition (2010).

patients whose tumours were positive were 42%, 32% and 49%, respectively. The prognostic significance of variant actinin-4 protein expression was reproducibly observed in subgroup analyses of patients with stages I and II and stages III and IV HGNT ($P = 0.0089$ and $P = 0.049$, respectively) (Figure 3C and D), whereas the expression of total actinin-4 proteins (detected by 13G9 monoclonal antibody) (supplementary Figure S4, available at *Annals of Oncology* online) or the three conventional NE markers (CGA, SYN and CD56) (supplementary Figure S5, available at *Annals of Oncology* online) did not show such prognostic significance.

Univariate analysis with the Cox proportional hazards model (Table 3) revealed that lymph node metastasis ($P = 0.000082$) and immunoreactivity for the actinin-4 splice variant ($P = 0.000467$) were significantly correlated with the outcome of the 173 patients with HGNTs. Multivariate analysis indicated that the expression of the actinin-4 splice variant was the most significant independent predictor of unfavourable outcome ($P = 0.00113$; hazard ratio (HR), 2.15; 95% confidence interval (CI) 1.36–3.40) after the presence of lymph node metastasis (P

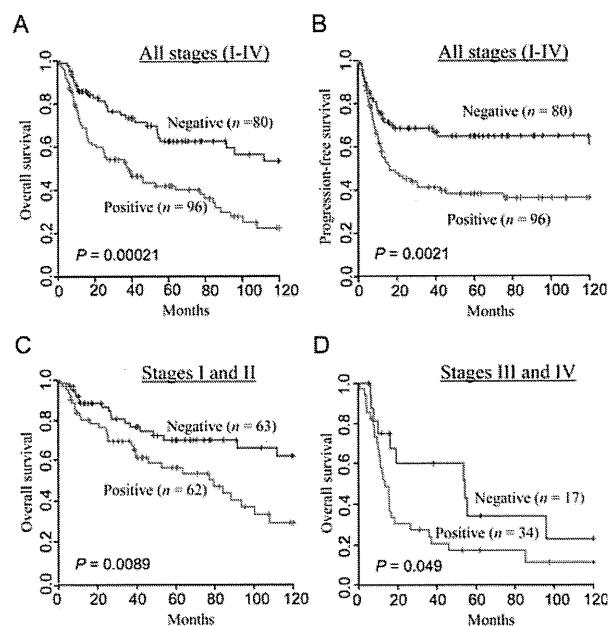


Figure 3. Survival of high-grade neuroendocrine tumour (HGNT) patients according to expression of the actinin-4 variant protein. Kaplan-Meier estimates of overall (A, C and D) and progression-free (B) survival for patients with all stages (A and B), stages I and II (C) and stages III and IV (D) HGNTs. Differences between the curves were assessed using the log-rank test.

$= 0.00023$; HR, 2.25; 95% CI 1.46–3.47). The variant actinin-4 protein expression was also a significant independent predictor of outcome for SCLC (supplementary Table S2, available at *Annals of Oncology* online) ($P = 0.050$; HR, 2.16; 95% CI 1.00–4.68) and LCNEC (supplementary Table S3, available at *Annals of Oncology* online) ($P = 0.0038$; HR, 2.37; 95% CI 1.32–4.26).

discussion

In this study, we first determined the distribution of expression of the alternatively spliced *ACTN4* transcript in a large panel of human cancer cell lines derived from various tissues. We confirmed the frequent expression of *ACTN4*-Va in SCLCs and the absence of its expression in NSCLCs. The variant transcript was also expressed frequently in choriocarcinoma, but its relationship with NE differentiation as well as its clinical significance remained undetermined. We then investigated the expression of the variant actinin-4 protein in a variety of histological subtypes of lung cancer using a newly established monoclonal antibody (Figure 1). We found that the expression pattern of the variant protein was apparently different from any of the conventional NE markers. CGA, SYN and CD56 were expressed in 76%–100% of pulmonary carcinoid tumours (Table 1), whereas the variant actinin-4 was expressed in only 10% (5/51) of them. The expression of variant actinin-4, but not that of CGA, SYN or CD56, was significantly associated with an unfavourable post-surgical outcome in HGNT patients (Figure 3 and supplementary Figure S5, available at *Annals of Oncology* online). These results indicated that variant actinin-4

Table 3. Hazard ratios for death in patients with high-grade neuroendocrine tumours

Variable	N	Univariate analysis			Multivariate analysis		
		HR	95% CI	P value	HR	95% CI	P value
Age							
< 65/≥65 years	71/102	1.00	0.65–1.55	0.983			
Smoking history							
Absent/present	7/166	1.63	0.40–6.65	0.492			
Gender							
Female/male	33/140	1.12	0.64–1.96	0.683			
Tumour size							
≤3 cm/>3 cm	93/80	1.33	0.87–2.04	0.184			
Lymph node metastasis							
Absent/present	101/72	2.37	1.54–3.65	0.00008	2.25	1.46–3.47	0.00023
Distant metastasis							
Absent/present	167/6	1.70	0.69–4.20	0.249			
Adjuvant chemotherapy							
Yes/no	40/133	0.77	0.44–1.35	0.362			
Histological subtype							
LCNEC/SCLC	103/70	1.12	0.73–1.74	0.596			
Variant actinin-4 protein expression							
Negative/positive	79/94	2.27	1.43–3.59	0.000467	2.15	1.36–3.40	0.00113

Three patients with LCNEC, for whom no data regarding adjuvant therapy were available, were excluded from the analysis. HR, hazard ratio; CI, confidence interval; LCNEC, large cell neuroendocrine carcinoma; SCLC, small cell lung carcinoma.

is not a simple marker for NE differentiation, but seems to be associated with the malignant progression of NE tumours.

We originally identified actinin-4 as an actin-bundling protein associated with enhanced cell motility and cancer invasion [9]. Actinin-4 directly regulates cell motility through remodelling of the actin cytoskeleton [9, 22]. Increased expression of actinin-4 protein is closely associated with a poor outcome in patients with breast cancer [9], colorectal cancer [22], pancreatic cancer [18], ovarian cancer [19] and NSCLC [23]. However, the expression of total actinin-4 protein (i.e. the ubiquitous and variant actinin-4 proteins together) detected by the monoclonal antibody 13G9 was not significantly correlated with the outcome of HGNT patients (supplementary Figure S4, available at *Annals of Oncology* online). The amino acid sequence encoded by exon 8 is crucial for the function of the *ACTN4* gene. In fact, a germline missense mutation in exon 8 is responsible for a hereditary renal disease, familial focal segmental glomerulosclerosis [24]. The splice variant as well as mutated actinin-4 proteins have a higher affinity for actin polymers [10]. SCLC shows an abnormal actin cytoskeleton structure [10]. Existing experimental data as well as the current clinical observations suggest that variant actinin-4 very likely plays a functional role in the aggressive behaviour of NE lung tumours. Because of its limited expression in normal tissues, variant actinin-4 may also serve as a therapeutic target.

If a biomarker capable of defining a subset of HGNT patients whose prognosis is likely to be unfavourable were to be identified, allowing them to be selected for intense adjuvant chemotherapy, then their survival might be improved. Recently Klotho was newly characterized as a biomarker predictive of a favourable outcome in patients with LCNEC [25] and limited-disease SCLC [26], although the number of cases examined was relatively small. The expression of CD117 was also

reported to show marginally significant correlation with recurrence of LCNEC ($P = 0.046$) [27]. It is expected that combination of these emerging prognostic biomarkers with variant actinin-4 would further improve the accuracy of HNGT prognostication. Future investigation to select and validate an optimal biomarker set is anticipated.

funding

This study was supported by the Program for Promotion of Fundamental Studies in Health Sciences conducted by the National Institute of Biomedical Innovation of Japan, Research on Biological Markers for New Drug Development conducted by the Ministry of Health, Labor and Welfare of Japan and the National Cancer Center Research and Development Fund.

disclosure

The authors have declared no conflicts of interest.

references

1. Travis WD, Linnoila RI, Tsokos MG et al. Neuroendocrine tumors of the lung with proposed criteria for large-cell neuroendocrine carcinoma. An ultrastructural, immunohistochemical, and flow cytometric study of 35 cases. *Am J Surg Pathol* 1991; 15: 529–553.
2. Travis WD, Colby TV, Corrin B et al. World Health Organization International Histological Classification of Tumors. Histological Typing of Lung and Pleural Tumors, 3rd edition. Berlin: Springer 1999.
3. Cooper WA, Thourani VH, Gal AA et al. The surgical spectrum of pulmonary neuroendocrine neoplasms. *Chest* 2001; 119: 14–18.
4. Travis WD, Rush W, Flieder DB et al. Survival analysis of 200 pulmonary neuroendocrine tumors with clarification of criteria for atypical carcinoid and its separation from typical carcinoid. *Am J Surg Pathol* 1998; 22: 934–944.

5. Asamura H, Kameya T, Matsuno Y et al. Neuroendocrine neoplasms of the lung: a prognostic spectrum. *J Clin Oncol* 2006; 24: 70–76.
6. Travis WD. Advances in neuroendocrine lung tumors. *Ann Oncol* 2010; 21(Suppl 7): vii65–vii71.
7. Takei H, Asamura H, Maeshima A et al. Large cell neuroendocrine carcinoma of the lung: a clinicopathologic study of eighty-seven cases. *J Thorac Cardiovasc Surg* 2002; 124: 285–292.
8. Ionescu DN, Treaba D, Gilks CB et al. Nonsmall cell lung carcinoma with neuroendocrine differentiation—an entity of no clinical or prognostic significance. *Am J Surg Pathol* 2007; 31: 26–32.
9. Honda K, Yamada T, Endo R et al. Actinin-4, a novel actin-bundling protein associated with cell motility and cancer invasion. *J Cell Biol* 1998; 140: 1383–1393.
10. Honda K, Yamada T, Seike M et al. Alternative splice variant of actinin-4 in small cell lung cancer. *Oncogene* 2004; 23: 5257–5262.
11. Pio R, Montuenga LM. Alternative splicing in lung cancer. *J Thorac Oncol* 2009; 4: 674–678.
12. Säkaguchi N, Kimura T, Matsushita S et al. Generation of high-affinity antibody against T-cell-dependent antigen in the Ganp gene-transgenic mouse. *J Immunol* 2005; 174: 4485–4494.
13. Ono M, Matsubara J, Honda K et al. Prolyl 4-hydroxylation of alpha-fibrinogen: a novel protein modification revealed by plasma proteomics. *J Biol Chem* 2009; 284: 29041–29049.
14. Matsubara J, Ono M, Negishi A et al. Identification of a predictive biomarker for hematologic toxicities of gemcitabine. *J Clin Oncol* 2009; 27: 2261–2268.
15. Satow R, Shtashige M, Jigami T et al. β -Catenin inhibits promyelocytic leukemia protein tumor suppressor function in colorectal cancer cells. *Gastroenterology* 2012; 142: 572–581.
16. Travis WD, Brambilla E, Muller-Hermelink HK. World Health Organization Classification of Tumours. Pathology and Genetics of Tumours of the Lung, Pleura, Thymus and Heart. Lyon: IARC Press 2004.
17. Sobin L, Gospodarowicz M, Wittrkind C. TNM Classification of Malignant Tumors. New York: Wiley-Blackwell 2010.
18. Kikuchi S, Honda K, Tsuda H et al. Expression and gene amplification of actinin-4 in invasive ductal carcinoma of the pancreas. *Clin Cancer Res* 2008; 14: 5348–5356.
19. Yamamoto S, Tsuda H, Honda K et al. Actinin-4 expression in ovarian cancer: a novel prognostic indicator independent of clinical stage and histological type. *Mod Pathol* 2007; 20: 1278–1285.
20. Idogawa M, Yamada T, Honda K et al. Poly(ADP-ribose) polymerase-1 is a component of the oncogenic T-cell factor-4/beta-catenin complex. *Gastroenterology* 2005; 128: 1919–1936.
21. Yamaguchi U, Nakayama R, Honda K et al. Distinct gene expression-defined classes of gastrointestinal stromal tumor. *J Clin Oncol* 2008; 26: 4100–4108.
22. Honda K, Yamada T, Hayashida Y et al. Actinin-4 increases cell motility and promotes lymph node metastasis of colorectal cancer. *Gastroenterology* 2005; 128: 51–62.
23. Yamagata N, Shyr Y, Yanagisawa K et al. A training-testing approach to the molecular classification of resected non-small cell lung cancer. *Clin Cancer Res* 2003; 9: 4695–4704.
24. Kaplan JM, Kim SH, North KN et al. Mutations in ACTN4, encoding alpha-actinin-4, cause familial focal segmental glomerulosclerosis. *Nat Genet* 2000; 24: 251–256.
25. Usuda J, Ichinose S, Ishizumi T et al. Klotho is a novel biomarker for good survival in resected large cell neuroendocrine carcinoma of the lung. *Lung Cancer* 2011; 72: 355–359.
26. Usuda J, Ichinose S, Ishizumi T et al. Klotho predicts good clinical outcome in patients with limited-disease small cell lung cancer who received surgery. *Lung Cancer* 2011; 74: 332–337.
27. Casali C, Stefani A, Rossi G et al. The prognostic role of c-kit protein expression in resected large cell neuroendocrine carcinoma of the lung. *Ann Thorac Surg* 2004; 77: 247–252.

Annals of Oncology 24: 90–96, 2013
doi:10.1093/annonc/mds281
Published online 16 August 2012

Phase Ib safety and pharmacokinetic study of volociximab, an anti- $\alpha 5\beta 1$ integrin antibody, in combination with carboplatin and paclitaxel in advanced non-small-cell lung cancer

B. Besse^{1*}, L. C. Tsao², D. T. Chao³, Y. Fang⁴, J.-C. Soria^{5,6}, S. Almokadem⁷ & C. P. Belani⁷

¹Cancer Medicine/Thoracic Unit, Institut Gustave Roussy, Villejuif, France; ²Departments of ³Biometry; ⁴Discovery, GPRD; ⁵Bio-analytical Sciences, Department of Preclinical and Clinical Development Sciences, Abbott Biotherapeutics Corp., Redwood City, USA; ⁶Cancer Medicine/Service des Innovations Thérapeutiques Précoces, Institut Gustave Roussy, Villejuif, France; ⁷Université Paris-Sud 11, Orsay, France; ⁷Department of Medicine, Division of Medical Oncology, Penn State Hershey Cancer Institute, Hershey, USA

Received 14 February 2012; revised 15 May 2012; accepted 20 June 2012

Background: This phase Ib study evaluated volociximab, an anti- $\alpha 5\beta 1$ integrin antibody, in combination with carboplatin (Eli Lilly and Co., Indianapolis, IN) and paclitaxel (Taxol) in advanced, untreated non-small-cell lung cancer (NSCLC).

*Correspondence to: Dr B. Besse, Department of Oncology Medicine/Thoracic Unit, Institut Gustave Roussy, Villejuif Cedex 94805, France. Tel: +33-1-42114322; Fax: +33-1-42-11-52-19; E-mail: benjamin.besse@igr.fr

Genome-wide DNA methylation profiles in liver tissue at the precancerous stage and in hepatocellular carcinoma

Eri Arai¹, Saori Ushijima¹, Masahiro Gotoh¹, Hidenori Ojima¹, Tomoo Kosuge², Fumie Hosoda³, Tatsuhiro Shibata³, Tadashi Kondo⁴, Sana Yokoi⁵, Issei Imoto⁵, Johji Inazawa⁵, Setsuo Hirohashi¹ and Yae Kanai^{1*}

¹Pathology Division, National Cancer Center Research Institute, Tokyo, Japan

²Hepatobiliary and Pancreatic Surgery Division, National Cancer Center Hospital, Tokyo, Japan

³Cancer Genomics Project, National Cancer Center Research Institute, Tokyo, Japan

⁴Proteome Bioinformatics Project, National Cancer Center Research Institute, Tokyo, Japan

⁵Department of Molecular Cytogenetics, Medical Research Institute and School of Biomedical Science, Tokyo Medical and Dental University, Tokyo, Japan

To clarify genome-wide DNA methylation profiles during hepatocarcinogenesis, bacterial artificial chromosome (BAC) array-based methylated CpG island amplification was performed on 126 tissue samples. The average numbers of BAC clones showing DNA hypo- or hypermethylation increased from noncancerous liver tissue obtained from patients with hepatocellular carcinomas (HCCs) (N) to HCCs. N appeared to be at the precancerous stage, showing DNA methylation alterations that were correlated with the future development of HCC. Using Wilcoxon test, 25 BAC clones, whose DNA methylation status was inherited by HCCs from N and were able to discriminate 15 N samples from 10 samples of normal liver tissue obtained from patients without HCCs (C) with 100% sensitivity and specificity, were identified. The criteria using the 25 BAC clones were able to discriminate 24 additional N samples from 26 C samples in the validation set with 95.8% sensitivity and 96.2% specificity. Using Wilcoxon test, 41 BAC clones, whose DNA methylation status was able to discriminate patients who survived more than 4 years after hepatectomy from patients who suffered recurrence within 6 months and died within a year after hepatectomy, were identified. The DNA methylation status of the 41 BAC clones was correlated with the cancer-free and overall survival rates of patients with HCC. Multivariate analysis revealed that satisfying the criteria using the 41 BAC clones was an independent predictor of overall outcome. Genome-wide alterations of DNA methylation may participate in hepatocarcinogenesis from the precancerous stage, and DNA methylation profiling may provide optimal indicators for carcinogenetic risk estimation and prognostication.

© 2009 UICC

Key words: bacterial artificial chromosome array-based methylated CpG island amplification; hepatocellular carcinoma; multistage carcinogenesis; precancerous condition; prognostication

Alteration of DNA methylation is one of the most consistent epigenetic changes in human cancers.^{1,2} It is known that DNA hypomethylation results in chromosomal instability as a result of changes in the chromatin structure, and that DNA hypermethylation of CpG islands silences tumor-related genes in cooperation with histone modification in human cancers.^{3,4}

With respect to hepatocarcinogenesis, we have shown that alterations of DNA methylation at multiple chromosomal loci can be detected even in noncancerous liver tissue showing chronic hepatitis or cirrhosis, which are widely considered to be precancerous conditions, but not in normal liver tissue, using classical Southern blotting analysis.⁵ This was one of the earliest reports of alterations of DNA methylation at the precancerous stage. Multiple tumor-related genes, such as the *E-cadherin*^{6,7} and *hypermethylated-in-cancer (HIC)-I*⁸ genes, are silenced by DNA hypermethylation in hepatocellular carcinomas (HCCs). DNA methyltransferase (DNMT) 1 expression is significantly higher even in noncancerous liver tissue showing chronic hepatitis or cirrhosis than in the normal liver tissue and is even higher in HCCs.^{9,10} DNMT1 overexpression is also correlated with poorer tumor differentiation, portal vein involvement and intrahepatic metastasis of HCCs and poorer patient outcome.¹¹ On the other hand, overexpression of DNMT3b4, an inactive splice

variant of DNMT3b, may lead to chromosomal instability through induction of DNA hypomethylation in pericentromeric satellite regions during hepatocarcinogenesis.¹²

Because aberrant DNA methylation is one of the earliest molecular events during hepatocarcinogenesis and also participates in malignant progression,^{13,14} it may be possible to estimate the future risk of developing more malignant HCCs on the basis of DNA methylation status. However, only a few previous studies focusing on HCCs have used recently developed array-based technology for assessing genome-wide DNA methylation status,¹⁵ and such studies have focused mainly on identification of tumor-related genes that are silenced by DNA methylation. DNA methylation profiles, which could become the optimum indicator for carcinogenetic risk estimation and prediction of patient outcome, should therefore be further explored during hepatocarcinogenesis using array-based approaches.

In this study, to clarify genome-wide DNA methylation profiles during multistage hepatocarcinogenesis, we performed bacterial artificial chromosome (BAC) array-based methylated CpG island amplification (BAMCA)^{16–18} using a microarray of 4,361 BAC clones¹⁹ in the normal liver tissue obtained from patients without HCCs, noncancerous liver tissue obtained from patients with HCCs, and in HCCs themselves.

Material and methods

Patients and tissue samples

As a learning cohort, 15 samples of the noncancerous liver tissue (N1 to N15) and 19 primary HCCs (T1 to T19) were obtained from surgically resected specimens from 16 patients who underwent partial hepatectomy at the National Cancer Center Hospital, Tokyo, Japan. The patients comprised 13 men and 3 women with a mean (\pm SD) age of 64.9 ± 7.4 years. Of these, 7 were positive for hepatitis B virus (HBV) surface antigen (HBs-Ag), 8 were positive for anti-hepatitis C virus (HCV) antibody (anti-HCV) and 1 was negative for both. Histological examination of the noncancerous liver tissue samples revealed findings compatible with chronic hepatitis in 5 and cirrhosis in 9 and no remarkable histological findings in 1.

Additional Supporting Information may be found in the online version of this article.

Grant sponsors: Ministry of Health, Labor and Welfare of Japan (Third Term Comprehensive 10-Year Strategy for Cancer Control and Cancer Research), New Energy and Industrial Technology Development Organization (NEDO), National Institute of Biomedical Innovation (NiBio) (Program for Promotion of Fundamental Studies in Health Sciences).

*Correspondence to: Pathology Division, National Cancer Center Research Institute, 5-1-1 Tsukiji, Chuo-ku, Tokyo 104-0045, Japan. Fax: +81-3-3248-2463. E-mail: ykanai@ncc.go.jp

Received 3 February 2009; Accepted after revision 25 June 2009

DOI 10.1002/ijc.24708

Published online 30 June 2009 in Wiley InterScience (www.interscience.wiley.com).

For the comparison, 10 normal liver tissue samples (C1 to C10) showing no remarkable histological findings were also obtained from 10 patients without HCCs who were both HBs-Ag- and anti-HCV-negative. The patients comprised 7 men and 3 women with a mean age of 58.4 ± 9.7 years. Nine patients underwent partial hepatectomy for liver metastases of primary colon cancers, and 1 patient did so for liver metastases of gastrointestinal stromal tumor of the stomach.

In addition, for the comparison, 7 liver tissue samples (V1 to V7) were obtained from 7 patients who were positive for HBs-Ag or anti-HCV, but who had never developed HCCs. The patients comprised 4 men and 3 women with a mean age of 62.4 ± 5.2 years. Three patients underwent partial hepatectomy for liver metastases of primary colon or rectal cancers, and 1 patient did so for liver metastases of gastric cancer. Three patients underwent partial hepatectomy for cholangiocellular carcinomas.

As a validation cohort, 26 normal liver tissue samples (C11 to C36) showing no remarkable histological features were obtained from 26 patients without HCCs who were both HBs-Ag- and anti-HCV-negative. Twenty-four noncancerous liver tissue samples (N16 to N 39) and 25 primary HCCs (T20 to T44) were obtained from surgically resected specimens from 24 patients who underwent partial hepatectomy were added. The patients from whom C11 to C36 were obtained comprised 21 men and 5 women with a mean age of 59.9 ± 10.9 years. The patients with HCCs from whom N16 to N 39 and T20 to T44 were obtained comprised 22 men and 2 women with a mean age of 61.6 ± 11.4 years. Of the 24 patients with HCCs from whom N16 to N 39 and T20 to T44 were obtained, 5 were positive for HBs-Ag, 16 were positive for anti-HCV and 3 were negative for both. Histological examination of N16 to N 39 revealed findings compatible with chronic hepatitis and cirrhosis in 16 and 8 samples, respectively.

This study was approved by the Ethics Committee of the National Cancer Center, Tokyo, Japan.

BAMCA

High molecular weight DNA from fresh-frozen tissue samples was extracted using phenol-chloroform followed by dialysis. Because DNA methylation status is known to be organ specific, the reference DNA for analysis of the developmental stages of HCCs should be obtained from the liver and not from other organs or peripheral blood. Therefore, a mixture of normal liver tissue DNA obtained from 5 male patients (C37 to C41) and 5 female patients (C42 to C46) was used as a reference for analyses of male and female test DNA samples, respectively.

DNA methylation status was analyzed by BAMCA using a custom-made array (MCG Whole Genome Array-4500) harboring 4,361 BAC clones located throughout chromosomes 1 to 22 and X and Y,¹⁶⁻¹⁸ as described previously. Briefly, 5- μ g aliquots of test or reference DNA were first digested with 100 units of methylation-sensitive restriction enzyme *Sma* I and subsequently with 20 units of methylation-insensitive *Xma* I. Adapters were ligated to *Xma* I-digested sticky ends, and polymerase chain reaction (PCR) was performed with an adapter primer set. Test and reference PCR products were labeled by random priming with Cy3- and Cy5-dCTP (GE Healthcare, Buckinghamshire, UK), respectively, and precipitated together with ethanol in the presence of Cot-I DNA. The mixture was applied to array slides and incubated at 43°C for 72 hr. Arrays were scanned with a GenePix Personal 4100A (Axon Instruments, Foster City, CA) and analyzed using GenePix Pro 5.0 imaging software (Axon Instruments) and Acue 2 software (Mitsui Knowledge Industry, Tokyo, Japan). The signal ratios were normalized in each sample to make the mean signal ratios of all BAC clones 1.0.

Statistics

Differences in the average number of BAC clones that showed DNA methylation alterations between groups of samples were analyzed using the Mann-Whitney *U* test or the Kruskal-Wallis test.

Correlations between DNA methylation alterations in noncancerous liver tissue samples and the incidence of metachronous development and recurrence of HCCs were analyzed using the chi-squared test. Differences at $p < 0.05$ were considered significant. BAC clones whose signal ratios yielded by BAMCA were significantly different between groups of samples were identified by Wilcoxon test ($p < 0.01$). A support vector machine algorithm and a leave-one-out cross-validation were used to identify BAC clones by which the cumulative error rate for discrimination of sample groups became minimal. Two-dimensional hierarchical clustering analysis of noncancerous liver tissue samples and the BAC clones, and such analysis of HCCs and the BAC clones, were performed using the Expressionist software program (Gene Data, Basel, Switzerland). Survival curves of patient groups with HCCs were calculated by the Kaplan-Meier method, and the differences were compared by the log-rank test. The Cox proportional hazards multivariate model was used to examine the prognostic impact of DNA methylation status, histological differentiation, portal vein tumor thrombi, intrahepatic metastasis and multicentricity. Differences at $p < 0.05$ were considered significant.

Results

Genome-wide DNA methylation alterations during multistage hepatocarcinogenesis

Figures 1a and 1b show examples of scanned array images and scattergrams of the signal ratios (test signal/reference signal), respectively, for normal liver tissue from a patient without HCC (Panel C), and both noncancerous liver tissue (Panel N) and cancerous tissue (Panel T) from a patient with HCC. In all normal liver tissue samples, the signal ratios of 97% of the BAC clones were between 0.67 and 1.5 (red bars in Fig. 1b). Therefore, in noncancerous liver tissue obtained from patients with HCCs and HCCs, DNA methylation status corresponding to a signal ratio of less than 0.67 and more than 1.5 was defined as DNA hypomethylation and DNA hypermethylation of each BAC clone compared with normal liver tissue, respectively.

In samples of noncancerous liver tissue obtained from patients with HCCs, many BAC clones showed DNA hypo- or hypermethylation (Panel N of Fig. 1b). In the learning cohort, all 9 patients (100%) showing DNA hypo- or hypermethylation on 70 or more than 70 BAC clones in their noncancerous liver tissue samples developed metachronous or recurrent HCCs after hepatectomy, whereas only 2 (30%) of the 6 patients showing DNA hypo- or hypermethylation on less than 70 BAC clones in their noncancerous liver tissue samples did so ($p = 0.0235$).

In HCCs themselves, more BAC clones showed DNA hypo- or hypermethylation, and the degree of DNA hypo- or hypermethylation, *i.e.*, deviation of the signal ratio from 0.67 or 1.5, was increased (Panel T of Fig. 1b) in comparison with noncancerous liver tissue obtained from patients with HCCs. The average numbers of BAC clones showing a signal ratio of less than 0.67 ($p = 0.0000063$) and more than 1.5 ($p = 0.00000052$) were increased significantly relative to normal liver tissue, to noncancerous liver tissue obtained from patients with HCCs, and to HCCs (Table I).

There were no significant differences in the number of BAC clones showing DNA hypo- or hypermethylation in samples of normal liver tissue obtained from male and female patients without HCCs (66.0 ± 30.1 and 98.7 ± 55.9 , $p = 0.362$) and noncancerous liver tissue (111.2 ± 68.4 and 60.7 ± 46.9 , $p = 0.279$) and cancerous tissue (521.5 ± 255.8 and 626.7 ± 329.0 , $p = 0.539$) obtained from male and female patients with HCCs, respectively. Although there were no significant differences in the number of BAC clones showing DNA hypo- or hypermethylation between HBV- and HCV-positive patients with HCCs in both noncancerous liver tissue (108.3 ± 80.5 and 98.4 ± 60.0 , $p = 1.000$) and cancerous tissue (475.6 ± 323.8 and 497.0 ± 247.8 , $p = 0.689$), Wilcoxon test ($p < 0.01$) identified BAC clones in which DNA methylation status differed significantly between HBV- and

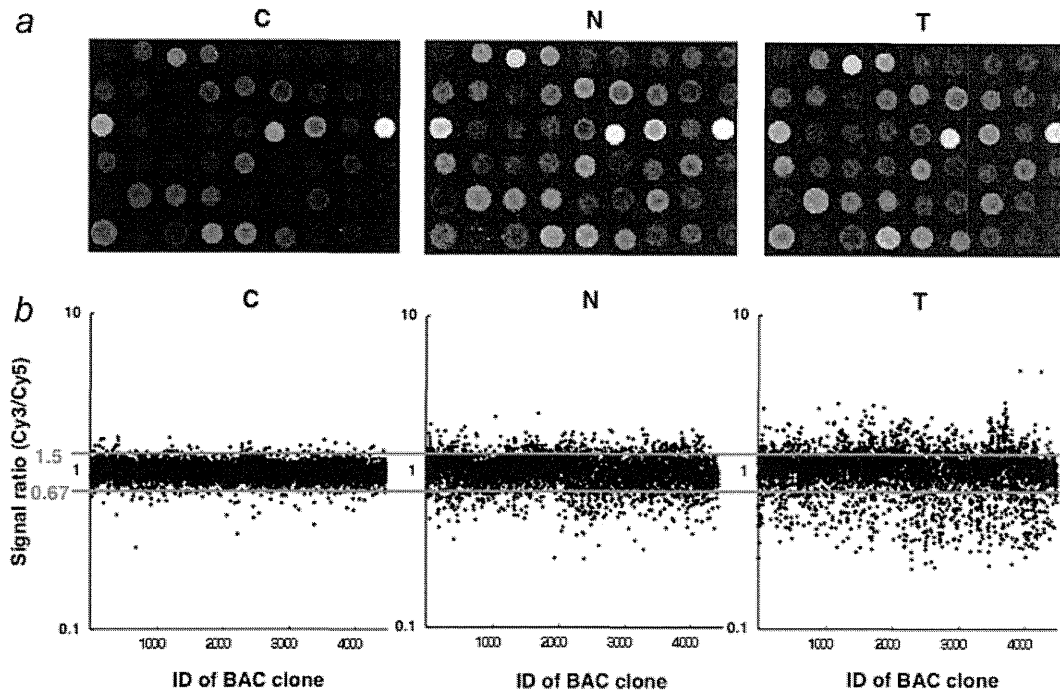


FIGURE 1 – Genome-wide DNA methylation alterations during multistage hepatocarcinogenesis. (a) Scanned array images yielded by BAMCA in normal liver tissue obtained from a patient without HCC (C) and noncancerous liver tissue (N) and cancerous tissue (T) obtained from a patient with HCC. (b) Scattergrams of the signal ratios yielded by BAMCA. In all C samples, the signal ratios of 97% of BAC clones were between 0.67 and 1.5 (red bars). In N and T, DNA methylation status corresponding to a signal ratio of less than 0.67 and more than 1.5 was defined as DNA hypomethylation and DNA hypermethylation on each BAC clone compared with C, respectively. Even in N, many BAC clones showed DNA hypo- or hypermethylation. In T, more BAC clones showed DNA hypo- or hypermethylation, and the degree of DNA hypo- or hypermethylation, *i.e.*, deviation of the signal ratio from 0.67 or 1.5 was increased in comparison with N.

TABLE 1 – GENOME-WIDE DNA METHYLATION ALTERATIONS DURING MULTISTAGE HEPATOCARCINOGENESIS

Tissue samples	Average number of BAC clones (mean \pm SD)					
	Signal ratio <0.67 (DNA hypomethylation)	<i>p</i>	Signal ratio >1.5 (DNA hypermethylation)	<i>p</i>	Signal ratio <0.67 or >1.5 (DNA hypo- or hypermethylation)	<i>p</i>
Normal liver tissue samples obtained from patient without HCCs (C, <i>n</i> = 10)	39.9 \pm 20.8	0.0000063 ¹	38.9 \pm 24.9	0.00000052 ¹	75.8 \pm 39.3	0.00000061 ¹
Noncancerous liver tissue samples obtained from patient with HCCs (N, <i>n</i> = 15)	61.2 \pm 46.8	0.000102 ²	39.9 \pm 27.3	0.0000026 ²	101.1 \pm 66.5	0.0000065 ²
HCCs (T, <i>n</i> = 19)	278.9 \pm 167.7	–	228.9 \pm 125.7	–	507.8 \pm 281.9	–

p values <0.05, which indicate significant differences.

¹Kruskal-Wallis test among C, N and T. ²Mann-Whitney *U* test between N and T.

HCV-positive patients with HCCs in noncancerous liver tissue (18 BAC clones) and cancerous tissue (15 BAC clones), respectively.

DNA methylation profiles discriminating noncancerous liver tissue obtained from patients with HCCs from normal liver tissue

The above findings indicating accumulation of clinicopathologically significant genome-wide DNA methylation alterations in noncancerous liver tissue prompted us to estimate the degree of carcinogenic risk based on DNA methylation profiles. Wilcoxon test (*p* < 0.01) revealed that the signal ratios of 512 BAC clones differed significantly between normal liver tissue samples and noncancerous liver tissue samples obtained from patients with HCCs. To omit potentially insignificant BAC clones associated only with inflammation and/or fibrosis and focus on BAC clones for which DNA methylation status was inherited by HCCs from the precancerous stage, we defined Groups I, II, III and IV. Group

I: BAC clones in which the average signal ratio of noncancerous liver tissue obtained from patients with HCCs was higher than that of normal liver tissue and the average signal ratio of HCCs was even higher than that of noncancerous liver tissue obtained from patients with HCCs (41 BAC clones), Group II: BAC clones in which the average signal ratio of noncancerous liver tissue obtained from patients with HCCs was higher than that of normal liver tissue and the average signal ratio of HCCs did not differ from that of noncancerous liver tissue obtained from patients with HCCs (146 BAC clones), Group III: BAC clones in which the average signal ratio of noncancerous liver tissue obtained from patients with HCCs was lower than that of normal liver tissue and the average signal ratio of HCCs was even lower than that of noncancerous liver tissue obtained from patients with HCCs (40 BAC clones), and Group IV: BAC clones in which the average signal ratio of noncancerous liver tissue obtained from patients with HCCs was lower than that of normal liver tissue and the average

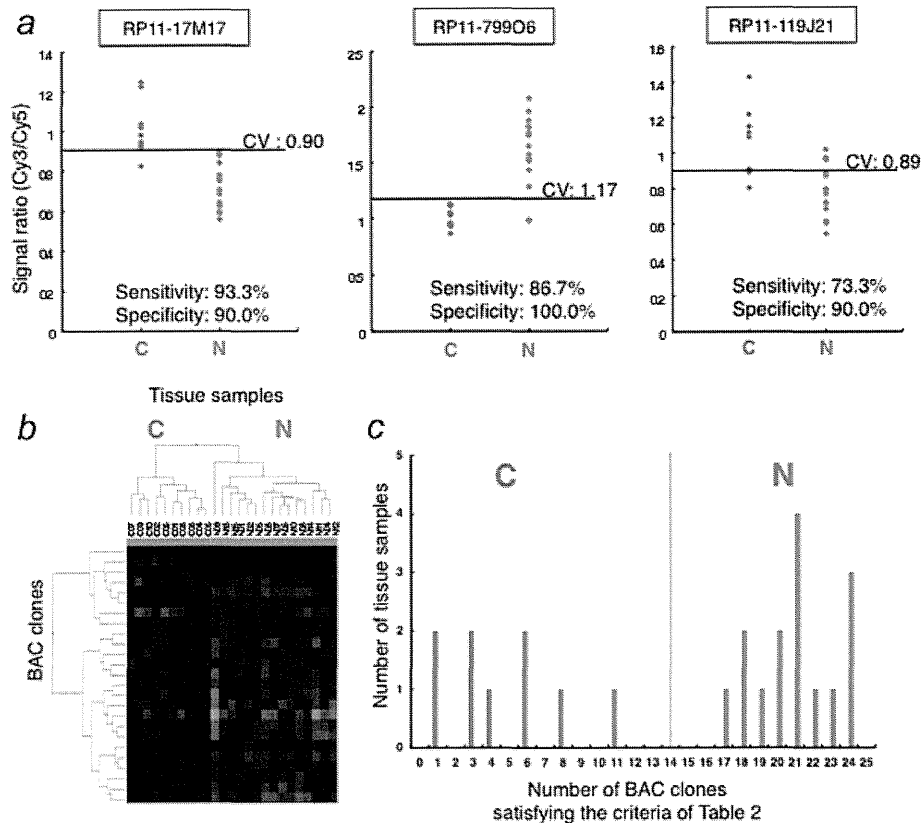


FIGURE 2 – DNA methylation profiles discriminating noncancerous liver tissue obtained from patients with HCCs from normal liver tissue. (a) Scattergrams of the signal ratios in normal liver tissue samples (C1 to C10) and noncancerous liver tissue samples obtained from patients with HCCs (N1 to N15) in the learning cohort on representative BAC clones, RP11-17M17, RP11-799O6 and RP11-119J21. Using the cutoff values (CV) described in each panel, noncancerous liver tissue samples obtained from patients with HCCs (N) in the learning cohort were discriminated from normal liver tissue samples (C) with sufficient sensitivity and specificity. (b) By 2-dimensional hierarchical clustering analysis using the 25 BAC clones selected by the process described in the Results section, normal liver tissue samples (C1 to C10) and noncancerous liver tissue samples obtained from patients with HCCs (N1 to N15) in the learning cohort were subclassified into the different subclasses without any error. The cluster trees for tissue samples and BAC clones are shown at the top and left of the panel, respectively. (c) Histogram showing the number of BAC clones satisfying the Table II criteria in samples C1 to C10 and N1 to N15. On the basis of this histogram, we established the following criteria: when the noncancerous liver tissue satisfied the criteria in Table II for 14 (green bar) or more than 14 BAC clones, it was judged to be at high risk of carcinogenesis.

signal ratio of HCCs did not differ from that of noncancerous liver tissue obtained from patients with HCCs (131 BAC clones). From the 512 BAC clones, 358 (Groups I, II, III and IV), in which the DNA methylation status was inherited by HCCs from noncancerous liver tissue, were selected. From the 358 BAC clones, the first 40 were identified by spot ranking analysis using the support vector machine algorithm for discrimination of noncancerous liver tissue obtained from patients with HCCs from normal liver tissue. Figure 2a shows scattergrams of the signal ratios in normal liver tissue samples and noncancerous liver tissue samples obtained from patients with HCCs on representative examples of the 40 BAC clones. Using the cutoff values described in each panel, noncancerous liver tissue obtained from patients with HCCs in the learning cohort was discriminated from normal liver tissue with sufficient sensitivity and specificity (Fig. 2a). From the 40 BAC clones, 25, for which such discrimination was performed with a sensitivity or specificity of 70% or more than 70%, were selected (Supporting Information Table S1). The cutoff values of the signal ratios for the 25 BAC clones, and their sensitivity and specificity, are shown in Table II. Two-dimensional hierarchical clustering analysis using the 25 BAC clones is shown in Figure 2b: 10 normal liver tissue samples (C1 to C10) and 15 noncancerous liver tissue samples obtained from patients with HCCs (N1 to N15) in the learning cohort were subclassified into different subclasses without any

error. The number of BAC clones satisfying the criteria listed in Table II in noncancerous liver tissue samples showing chronic hepatitis (20.6 ± 1.8) was not significantly different from that showing cirrhosis (21.3 ± 2.4 , $p = 0.542$) in the learning cohort.

A histogram showing the number of BAC clones satisfying the criteria listed in Table II for samples C1 to C10 and N1 to N15 is shown in Figure 2c. On the basis of this figure, we finally established the following criteria: when noncancerous liver tissue satisfied the criteria of Table II for 14 or more BAC clones (green bar in Fig. 2c), it was judged to be at high risk of carcinogenesis, and when noncancerous liver tissue satisfied the criteria of Table II for less than 14 BAC clones, it was judged not to be at high risk of carcinogenesis. Based on these criteria, both the sensitivity and specificity for diagnosis of noncancerous liver tissue samples obtained from patients with HCCs in the learning cohort as being at high risk of carcinogenesis were 100%.

To confirm these criteria, an additional 50 liver tissue samples were analyzed by BAMCA as a validation study (Supporting Information Figure S1). Twenty-three of 24 validation samples satisfying the criteria of Table II for 14 or more BAC clones were noncancerous liver tissue samples obtained from patients with HCCs (N16 to N36 and N38), and 24 of 26 validation samples satisfying the criteria of Table II for less than 14 BAC clones were normal

TABLE II - 25 BAC CLONES WHICH COULD DISCRIMINATE NONCANCEROUS LIVER TISSUES (N) FROM NORMAL LIVER TISSUES (C)

BAC clone ID	Location	Cutoff value	DNA methylation status ¹	Sensitivity (%)	Specificity (%)
RP11-104J13	1p35-1p36	1.01	C>N	93.3	70.0
RP11-52I2	1p34-1p35	1.00	C<N	80.0	60.0
RP11-29M22	1p11-1p12	1.11	C<N	86.7	90.0
RP11-21K1	2q37.2	1.00	C>N	86.7	70.0
RP11-109B15	5q33	1.04	C<N	66.7	90.0
RP11-88B24	6q26	0.95	C>N	80.0	70.0
RP11-112B7	7p13-7p14	1.00	C>N	80.0	70.0
RP11-48D21	8p11.2	1.00	C>N	80.0	90.0
RP11-120E20	11p15.4-11p15.5	0.90	C>N	73.3	100.0
RP11-334E6	11q23	1.00	C>N	86.7	80.0
RP11-17M17	11q25	0.90	C>N	93.3	90.0
RP11-319E16	12p13.32a	1.00	C>N	80.0	90.0
RP11-1100L3	12q13.13c-12q13.13d	1.04	C<N	86.7	80.0
RP11-799O6	12q13.3a-12q13.3b	1.17	C<N	86.7	100.0
RP11-119J21	12q24.33	0.89	C>N	73.3	90.0
RP11-332N6	14q11.2b	0.95	C>N	86.7	100.0
RP11-529E4	14q12c	1.00	C>N	93.3	50.0
RP11-89M4	16p13.2-16p13.3	1.20	C<N	86.7	100.0
RP11-215M5	15q15-15q21.1	1.00	C<N	86.7	70.0
RP11-348B12	19p13	1.00	C<N	80.0	80.0
RP11-134G22	20p11.2-20p12	1.01	C>N	80.0	90.0
RP11-328M17	22q13.2-22q13.33	0.93	C>N	86.7	100.0
RP11-354I12	22q13.31-22q13.33	1.00	C>N	93.3	80.0
RP11-55J11	22q13.2-22q13.33	1.00	C>N	80.0	70.0
RP11-480M11	Xq27.1-Xq28	0.90	C>N	80.0	90.0

¹C>N, when the signal ratio was lower than the cutoff value, the tissue sample was considered to be at high risk for carcinogenesis; C<N, when the signal ratio was higher than the cutoff value, the tissue sample was considered to be at high risk for carcinogenesis.

liver tissue samples (C11 to C31, 33, 34 and 36). That is, our criteria enabled diagnosis of noncancerous liver tissue samples obtained from patients with HCCs in the validation set as being at high risk of carcinogenesis with a sensitivity of 95.8% and a specificity of 96.2%. The number of BAC clones satisfying the criteria listed in Table II in noncancerous liver tissue samples showing chronic hepatitis (17.6 ± 2.5) was not significantly different from that showing cirrhosis (19.4 ± 1.8 , $p = 0.128$) in the validation cohort.

In addition, the average number of BAC clones satisfying the criteria in Table II was significantly lower in 7 samples of liver tissue obtained from patients who were infected with HBV or HCV, but who had never developed HCCs (V1 to V7, 13.14 ± 4.78), than that in N1 to N39 (19.21 ± 2.67 , $p = 0.00419$).

Association of HCC DNA methylation profiles with patient outcome

To establish criteria for prognostication of patients with HCCs, in the learning cohort, 5 of 19 HCC samples obtained from patients who had survived more than 4 years after hepatectomy and 6 of 19 HCC samples from patients who had suffered recurrence within 6 months and died within a year after hepatectomy were defined as a favorable-outcome group and a poor-outcome group, respectively. Wilcoxon test ($p < 0.01$) revealed that the signal ratios of 41 BAC clones (Supporting Information Table S1) differed significantly between the favorable-outcome group ($n = 5$) and the poor-outcome group ($n = 6$). Figure 3a shows scattergrams of the signal ratios in samples from the favorable- and poor-outcome groups for representative examples of the 41 BAC clones. Using the cutoff values described in Figure 3a and Table III for the 41 BAC clones, samples from the poor-outcome group were discriminated from favorable-outcome group samples with sufficient sensitivity and specificity (Fig. 3a and Table III). Two-dimensional hierarchical clustering analysis using the 41 BAC clones is shown in Figure 3b: 5 HCCs in the favorable-outcome group and 6 HCCs in the poor-outcome group were subclassified into different subclasses without any error (Fig. 3b). A histogram showing the number of BAC clones satisfying the criteria in Table III is shown in Fig. 3c. In all

19 HCCs in the learning cohort, multivariate analysis revealed that satisfying the criteria in Table III for 32 or more BAC clones was a predictor of overall patient outcome and was independent of parameters that are already known to have prognostic impact,²⁰ such as histological differentiation, portal vein tumor thrombi, intrahepatic metastasis and multicentricity (Table IV).

To confirm these criteria, an additional 25 HCC samples were analyzed by BAMCA as a validation study, and then evaluated based on the criteria in Table III. All 44 HCCs were divided into 2 groups according to the number of BAC clones satisfying the criteria (32 or more BAC clones vs. less than 32 BAC clones). The period covered ranged from 11 to 3,413 days (mean, 1,349 days). The cancer-free and overall survival rates of patients with HCCs satisfying the criteria in Table III for 32 or more BAC clones was significantly lower than that of patients with HCCs satisfying the criteria in Table III for less than 32 BAC clones (Fig. 3d, $p = 0.000000002$ and $p = 0.0013$, respectively).

Discussion

Although many researchers in the field of cancer epigenetics use promoter arrays to identify the genes that are methylated in cancer cells,²¹⁻²³ we used a BAC array¹⁹ in this study. The efficiency of identification of specific genes that are silenced by DNA methylations around the promoter regions and may become a target of therapy may be generally lower using the BAMCA approach than with conventional promoter array-based analysis. However, the promoter regions of specific genes are not the only target of DNA methylation alterations in human cancers. DNA methylation status in genomic regions not directly participating in gene silencing, such as the edges of CpG islands, may be altered at the precancerous stage before the alterations of the promoter regions themselves occur.²⁴ Moreover, aberrant DNA methylation of large regions of chromosomes, which are regulated in a coordinated manner in human cancers due to a process of long-range epigenetic silencing, has recently attracted attention.²⁵ BAMCA methods may be suitable for overviewing the DNA methylation status of individual large regions among all chromosomes and for

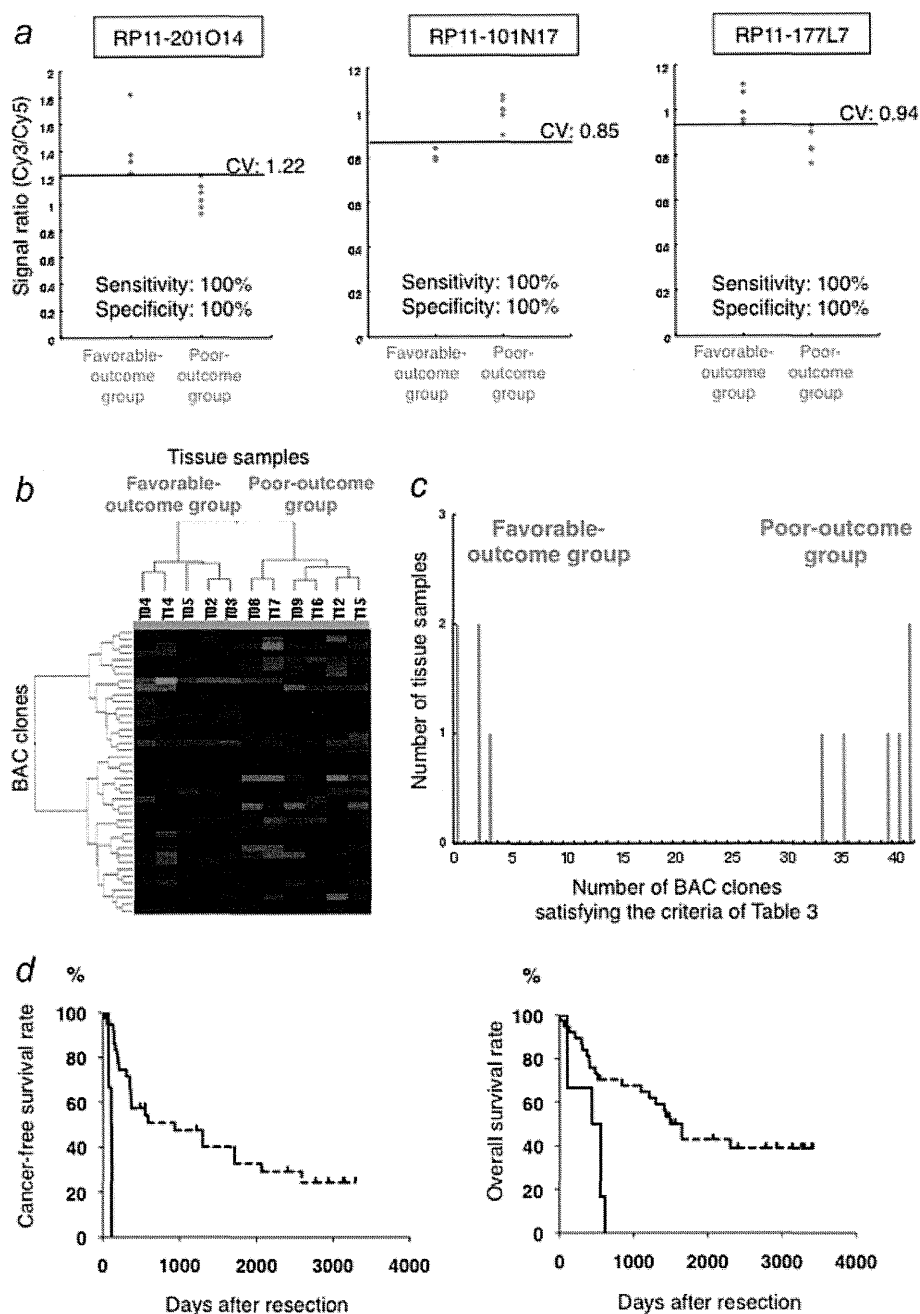


FIGURE 3 – DNA methylation profiles in HCCs associated with patient outcome. (a) Scattergrams of the signal ratios in HCCs from patients who survived more than 4 years after hepatectomy (favorable-outcome group, $n = 5$) and HCCs from patients who suffered recurrence within 6 months and died within a year after hepatectomy (poor-outcome group, $n = 6$) in the learning cohort for representative BAC clones, RP11-201O14, RP11-101N17 and RP11-177L7. Using the described cutoff values (CV), the poor-outcome group was discriminated from the favorable-outcome group with 100% sensitivity and specificity. (b) By 2-dimensional hierarchical clustering analysis using the 41 BAC clones selected by Wilcoxon test, HCCs in the favorable-outcome group and those in the poor-outcome group in the learning cohort were subclassified in the different subclasses without any error. The cluster trees for tissue samples and BAC clones are shown at the top and left of the panel, respectively. (c) Histogram showing the number of BAC clones satisfying the Table III criteria in HCCs of the favorable- and poor-outcome groups in the learning cohort. (d) Kaplan-Meier survival curves of all patients with HCCs (T1 to T44). The cancer-free (left panel, $p = 0.000000002$) and overall (right panel, $p = 0.0013$) survival rates of patients with HCCs satisfying the Table III criteria for 32 or more than 32 BAC clones (solid lines) were significantly lower than that of patients with HCCs satisfying the Table III criteria for less than 32 BAC clones (broken lines).

TABLE III – 41 BAC CLONES WHICH COULD DISCRIMINATE HCCS IN POOR-OUTCOME GROUP (P) FROM THOSE IN FAVORABLE-OUTCOME GROUP (F)

BAC clone ID	Location	Cutoff value	DNA methylation status ¹	Sensitivity (%)	Specificity (%)
RP11-89K16	1p35	1.50	F<P	83.3	100.0
RP11-201O14	1p34.3-1p36.13	1.22	F>P	100.0	100.0
RP11-156K6	1p31.1-1p31.3	1.15	F>P	100.0	80.0
RP11-553K8	1q31.2-1q31.3	1.16	F>P	100.0	100.0
RP11-89E10	1q31.3	0.91	F<P	100.0	100.0
RP11-180L21	2p16-2p21	1.29	F>P	100.0	80.0
RP11-90B13	2p14-2p15	1.13	F>P	83.3	100.0
RP11-449B19	2q11.2	0.75	F<P	100.0	80.0
RP11-30M1	2q32.3	1.10	F<P	100.0	100.0
RP11-89B13	2q32.3-2q33.1	1.11	F>P	83.3	80.0
RP11-255O19	3p24.3-3p25	1.08	F>P	100.0	100.0
RP11-421F9	3p24.2a	0.97	F>P	83.3	100.0
RP11-122D19	3p21.2	0.99	F<P	100.0	80.0
RP11-36K8	4q22	0.91	F>P	83.3	100.0
RP11-101N17	4q26	0.85	F<P	100.0	100.0
RP11-177L7	4q32	0.94	F>P	100.0	100.0
RP11-13O14	4q34-4q35	0.88	F<P	83.3	100.0
RP11-88H16	5p14	0.85	F<P	100.0	100.0
RP11-91G9	5q22-5q23	1.45	F<P	83.3	100.0
RP11-79K22	6q16	0.98	F<P	83.3	100.0
RP11-126B8	7q21.3	1.06	F>P	100.0	100.0
RP11-89P11	7q35	0.83	F>P	83.3	100.0
RP11-88N8	8q21.11d	1.02	F>P	100.0	100.0
RP11-85C21	9q33.3-9q34.2	0.95	F<P	83.3	100.0
RP11-714M16	10q26.11-10q26.3	1.00	F<P	100.0	100.0
RP11-48A2	10q26.2	0.69	F<P	100.0	80.0
RP11-206I1	11p11.2	1.20	F<P	100.0	100.0
RP11-35F11	11q12	1.30	F<P	100.0	80.0
RP11-158I9	11q23	1.04	F>P	83.3	100.0
RP11-74I8	12q13	1.13	F<P	100.0	100.0
RP11-167B4	16p13.3	0.97	F>P	83.3	100.0
RP11-368N21	16p11.2-16p12	1.10	F>P	83.3	100.0
RP11-303G21	16q12.1b	0.80	F>P	83.3	100.0
RP11-151M19	16q22	1.05	F>P	100.0	100.0
RP11-135N5	17p13.2	1.00	F>P	100.0	100.0
RP11-398A1	17q11.2d	1.00	F>P	100.0	100.0
RP11-15A1	19q13	1.08	F>P	83.3	100.0
RP11-697B10	19q13.3	0.90	F>P	83.3	100.0
RP11-79A3	19q13.3	1.05	F<P	100.0	100.0
RP11-29H19	20q12	1.00	F>P	100.0	100.0
RP11-36N5	22q11.2	1.15	F>P	83.3	100.0

¹F>P, when the signal ratio was lower than the cutoff value, the tissue sample was considered to have been obtained from a patient with poor prognosis; F<P, when the signal ratio was higher than the cutoff value, the tissue sample was considered to have been obtained from a patient with poor prognosis.

identifying reproducible indicators for carcinogenetic risk estimation and prognostication. In fact, we have successfully obtained optimal indicators for carcinogenetic risk estimation and prognostication of renal cell carcinomas²⁶ and urothelial carcinomas (data will be published elsewhere) by BAMCA using the same array as that used in this study.

Our previous studies indicated that alterations of DNA methylation are one of the earliest events of multistage hepatocarcinogenesis and participate in malignant progression of HCCs.^{5,7-14,27-29} However, since in previous studies we examined DNA methylation status on only a restricted number of CpG islands or chromosomal loci, it has not yet been clarified whether DNA methylation status on only restricted regions is simply altered at the precancerous stage, or whether genome-wide alterations of DNA methylation status have certain clinicopathological significance. As shown in Panel N of Figure 1b, genome-wide DNA methylation alterations (both hypo- and hypermethylation) were confirmed even in noncancerous liver tissue samples obtained from patients with HCCs. The number of BAC clones showing DNA methylation alterations and the degree of DNA methylation alterations were found to increase stepwise from the precancerous stage to the HCC stage (Fig. 1b and Table I). This study revealed that alterations of DNA methylation during

multistage hepatocarcinogenesis occur in a genome-wide manner. Genome-wide DNA methylation alterations may participate in multistage hepatocarcinogenesis potentially through the induction of chromosomal instability and silencing of tumor-suppressor genes. DNA methylation alterations in noncancerous liver tissue were correlated with the future development of HCCs, suggesting that DNA methylation alterations at the precancerous stage may not occur randomly but are prone to further accumulation of genetic and epigenetic alterations.

Although mass vaccination against HBV has been initiated, this will not have a major impact for many years, as the age at presentation of HBV is older than 50 years mainly in Asia and Africa.³⁰ The spread of HCV in Japan that occurred in the 1950s and 1960s has resulted in a rapid increase in the incidence of HCC since 1980. In other countries including the United States, where HCV infection spread more recently, an increase in the incidence of HCC is imminent.³¹ Although there were no significant differences in the number of BAC clones showing DNA hypo- or hypermethylation between HBV- and HCV-positive patients with HCCs, Wilcoxon test identified BAC clones in which DNA methylation status differed significantly between HBV- and HCV-positive patients with HCCs in both noncancerous liver tissue and cancerous tissue, suggesting that the HBV-related carcinogenetic

TABLE IV – MULTIVARIATE ANALYSIS OF CLINICOPATHOLOGICAL PARAMETERS AND DNA METHYLATION PROFILES ASSOCIATED WITH OVERALL OUTCOME IN PATIENTS WITH HCCS

Parameters	Hazard ratio (95% CI)	χ^2	<i>p</i>
Histological differentiation			
Well differentiated	1 (Reference)	0.031	0.8594
Moderately or poorly differentiated	0.817 (0.088-7.616)		
Portal vein tumor thrombi			
Negative	1 (Reference)	2.095	0.1478
Positive	4.474 (0.588-34.033)		
Intrahepatic metastasis ¹			
Negative	1 (Reference)	0.090	0.7647
Positive	1.248 (0.292-5.336)		
Multicentricity ¹			
Negative	1 (Reference)	1.499	0.2209
Positive	0.328 (0.055-1.955)		
The criteria of Table 3			
Satisfying for less than 32 BAC clones	1 (Reference)	4.997	0.0254
Satisfying for 32 or more BAC clones	4.466 (1.202-16.585)		

CI, confidence interval.

¹In patients with multiple lesions, whether the lesions other than the main tumor from which tissue samples were obtained for this study were intrahepatic metastases of the main tumor or second primary lesions was judged by microscopic observation of hepatectomy specimens based on the previously described criteria.³⁵

pathway may result in distinct DNA methylation profiles. These findings are in accordance with a previous report showing that HBV-related proteins can induce DNA methylation alterations.³²

The effectiveness of surgical resection for HCC is limited, unless the disease is diagnosed early at the asymptomatic stage. Therefore, surveillance at the precancerous stage will become a priority. To reveal the baseline liver histology, microscopic examination of liver biopsy specimens is performed in patients with HBV or HCV infection prior to interferon therapy.^{33,34} Therefore, carcinogenetic risk estimation using such liver biopsy specimens will be advantageous for close follow-up of patients who are at high risk of HCC development. Because even subtle alterations of DNA methylation profiles at the precancerous stage are stably preserved on DNA double strands by covalent bonds, they may be better indicators for risk estimation than mRNA and protein expression profiles that can be easily affected by the microenvironment of precursor cells.

The present genome-wide analysis revealed DNA methylation profiles that were able to discriminate noncancerous liver tissue obtained from patients with HCCs from normal liver tissue and diagnose it at high risk of HCC development in the learning set. The sensitivity and specificity in the validation set were 95.8 and 96.2%, respectively, and the criteria listed in Table II were validated. For carcinogenetic risk estimation using liver biopsy specimens obtained prior to interferon therapy, DNA methylation profiles actually associated with carcinogenesis should be discriminated from those associated with inflammation and/or fibrosis. Therefore, we first omitted potentially insignificant BAC clones

associated only with inflammation and/or fibrosis and focused on BAC clones for which DNA methylation status was inherited by HCCs from the precancerous stage (Groups I, II, III and IV). In fact, it was confirmed that there were no significant differences in the number of BAC clones satisfying the criteria in Table II between noncancerous liver tissue samples showing chronic hepatitis and noncancerous liver tissue samples showing cirrhosis, not only in the learning set ($p = 0.542$) but also in the validation set ($p = 0.128$), indicating that our criteria were not associated with the degree of inflammation or fibrosis. In addition, the average numbers of BAC clones satisfying the criteria in Table II were significantly lower in liver tissue of patients without HCCs (V1 to V7) than in noncancerous liver tissue of patients with HCCs (N1 to N39), even though the patients from whom V1 to V7 were obtained were infected with HBV or HCV. Therefore, our criteria not only discriminate noncancerous liver tissue obtained from patients with HCCs from normal liver tissue but may also be applicable for classifying liver tissue obtained from patients who are followed up because of HBV or HCV infection, chronic hepatitis or cirrhosis into that which may generate HCCs and that which will not. Our criteria are applicable to both patients with chronic hepatitis and liver cirrhosis, although liver cirrhosis is known to show a more pronounced tendency to lead to HCC development than chronic hepatitis.²⁰ We intend to validate the reliability of such risk estimation prospectively using liver biopsy specimens obtained prior to interferon therapy from a large cohort of patients. On the basis of the present data, we now consider it justifiable to propose that clinicians can apply a portion of biopsy cores for this type of prospective study.

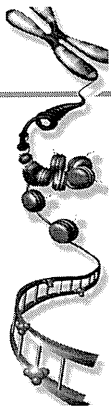
Because a sufficient quantity of good-quality DNA can be obtained from liver biopsy specimens, PCR-based analyses focusing on individual CpG sites are not always required. Although cut-off values should be modified for widely available standardized reference DNA, array-based analysis that overviews aberrant DNA methylation in each BAC region is immediately applicable to routine laboratory examinations. Moreover, because DNA methylation status of CpG sites is often regulated in a coordinated manner in each individual large region on chromosomes,^{13,14,25} an overview of the DNA methylation tendency (hypo- or hypermethylation) in the whole BAC region can be a more reproducible diagnostic indicator than one focusing on individual CpG sites.

The present genome-wide analysis revealed DNA methylation profiles that were able to discriminate a poor-outcome group from a favorable-outcome group. Correlation between the DNA methylation profiles and both cancer-free and overall survival rates of patients with HCCs (Fig. 3d) validated the criteria in Table III. Prognostication based on our criteria may be promising for supportive use during follow-up after surgical resection, because multivariate analysis revealed that our criteria can predict overall patient outcome independently of parameters observed in hepatectomy specimens that are already known to have prognostic impact.²⁰ Such prognostication using liver biopsy specimens obtained before transarterial embolization, transarterial chemoembolization and radiofrequency ablation may be advantageous even to patients who undergo such therapies. The reliability of such prognostication needs to be validated again prospectively in surgically resected specimens or biopsy specimens.

References

- Jones PA, Baylin SB. The fundamental role of epigenetic events in cancer. *Nat Rev Genet* 2002;3:415–28.
- Gronbaek K, Hother C, Jones PA. Epigenetic changes in cancer. *APMIS* 2007;115:1039–59.
- Eden A, Gaudet F, Waghmare A, Jaenisch R. Chromosomal instability and tumors promoted by DNA hypomethylation. *Science* 2003;300:455.
- Baylin SB, Ohm JE. Epigenetic gene silencing in cancer—a mechanism for early oncogenic pathway addiction? *Nat Rev Cancer* 2006;6:107–16.
- Kanai Y, Ushijima S, Tsuda H, Sakamoto M, Sugimura T, Hirohashi S. Aberrant DNA methylation on chromosome 16 is an early event in hepatocarcinogenesis. *Jpn J Cancer Res* 1996;87:1210–7.
- Yoshiura K, Kanai Y, Ochiai A, Shimoyama Y, Sugimura T, Hirohashi S. Silencing of the E-cadherin invasion-suppressor gene by CpG methylation in human carcinomas. *Proc Natl Acad Sci USA* 1995;92:7416–9.
- Kanai Y, Ushijima S, Hui AM, Ochiai A, Tsuda H, Sakamoto M, Hirohashi S. The E-cadherin gene is silenced by CpG methylation in human hepatocellular carcinomas. *Int J Cancer* 1997;71:355–9.
- Kanai Y, Hui AM, Sun L, Ushijima S, Sakamoto M, Tsuda H, Hirohashi S. DNA hypermethylation at the D17S5 locus and reduced HIC-1

- mRNA expression are associated with hepatocarcinogenesis. *Hepatology* 1999;29:703–9.
9. Sun L, Hui AM, Kanai Y, Sakamoto M, Hirohashi S. Increased DNA methyltransferase expression is associated with an early stage of human hepatocarcinogenesis. *Jpn J Cancer Res* 1997;88:1165–70.
 10. Saito Y, Kanai Y, Sakamoto M, Saito H, Ishii H, Hirohashi S. Expression of mRNA for DNA methyltransferases and methyl-CpG-binding proteins and DNA methylation status on CpG islands and pericentromeric satellite regions during human hepatocarcinogenesis. *Hepatology* 2001;33:561–8.
 11. Saito Y, Kanai Y, Nakagawa T, Sakamoto M, Saito H, Ishii H, Hirohashi S. Increased protein expression of DNA methyltransferase (DNMT) 1 is significantly correlated with the malignant potential and poor prognosis of human hepatocellular carcinomas. *Int J Cancer* 2003;105:527–32.
 12. Saito Y, Kanai Y, Sakamoto M, Saito H, Ishii H, Hirohashi S. Overexpression of a splice variant of DNA methyltransferase 3b, DNMT3b4, associated with DNA hypomethylation on pericentromeric satellite regions during human hepatocarcinogenesis. *Proc Natl Acad Sci USA* 2002;99:10060–5.
 13. Kanai Y, Hirohashi S. Alterations of DNA methylation associated with abnormalities of DNA methyltransferases in human cancers during transition from a precancerous to a malignant state. *Carcinogenesis* 2007;28:2434–42.
 14. Kanai Y. Alterations of DNA methylation and clinicopathological diversity of human cancers. *Pathol Int* 2008;58:544–58.
 15. Gao W, Kondo Y, Shen L, Shimizu Y, Sano T, Yamao K, Natsume A, Goto Y, Ito M, Murakami H, Osada H, Zhang J, et al. Variable DNA methylation patterns associated with progression of disease in hepatocellular carcinomas. *Carcinogenesis* 2008; 29:1901–10.
 16. Misawa A, Inoue J, Sugino Y, Hosoi H, Sugimoto T, Hosoda F, Ohki M, Imoto I, Inazawa J. Methylation-associated silencing of the nuclear receptor 112 gene in advanced-type neuroblastomas, identified by bacterial artificial chromosome array-based methylated CpG island amplification. *Cancer Res* 2005;65:10233–42.
 17. Sugino Y, Misawa A, Inoue J, Kitagawa M, Hosoi H, Sugimoto T, Imoto I, Inazawa J. Epigenetic silencing of prostaglandin E receptor 2 (PTGER2) is associated with progression of neuroblastomas. *Oncogene* 2007;26:7401–13.
 18. Tanaka K, Imoto I, Inoue J, Kozaki K, Tsuda H, Shimada Y, Aiko S, Yoshizumi Y, Iwai T, Kawano T, Inazawa J. Frequent methylation-associated silencing of a candidate tumor-suppressor, CRABP1, in esophageal squamous-cell carcinoma. *Oncogene* 2007;26:6456–68.
 19. Inazawa J, Inoue J, Imoto I. Comparative genomic hybridization (CGH)-arrays pave the way for identification of novel cancer-related genes. *Cancer Sci* 2004;95:559–63.
 20. Hirohashi S, Ishak KG, Kojiro M, Wanless IR, These ND, Tsukuma H, Blum HE, Deugnier Y, Puig PL, Fischer HP, Sakamoto M. Hepatocellular carcinoma. In: Hamilton SR, Altonen LA, eds. *World Health Organization classification of tumours. Pathology and genetics. Tumours of the digestive system*. Lyon: IARC Press, 2000. 159–72.
 21. Estecio MR, Yan PS, Ibrahim AE, Tellez CS, Shen L, Huang TH, Issa JP. High-throughput methylation profiling by MCA coupled to CpG island microarray. *Genome Res* 2007;17:1529–36.
 22. Jacinto FV, Ballestar E, Ropero S, Esteller M. Discovery of epigenetically silenced genes by methylated DNA immunoprecipitation in colon cancer cells. *Cancer Res* 2007;67:11481–6.
 23. Nielander I, Bug S, Richter J, Giefing M, Martin-Subero JI, Siebert R. Combining array-based approaches for the identification of candidate tumor suppressor loci in mature lymphoid neoplasms. *APMIS* 2007;115:1107–34.
 24. Maekita T, Nakazawa K, Mihara M, Nakajima T, Yanaoka K, Iguchi M, Arai K, Kaneda A, Tsukamoto T, Tatematsu M, Tamura G, Saito D, et al. High levels of aberrant DNA methylation in *Helicobacter pylori*-infected gastric mucosae and its possible association with gastric cancer risk. *Clin Cancer Res* 2006;12:989–95.
 25. Frigola J, Song J, Storzaker C, Hinshelwood RA, Peinado MA, Clark SJ. Epigenetic remodeling in colorectal cancer results in coordinate gene suppression across an entire chromosome band. *Nat Genet* 2006; 38:540–9.
 26. Arai E, Ushijima S, Fujimoto H, Hosoda F, Shibata T, Kondo T, Yokoi S, Imoto I, Inazawa J, Hirohashi S, Kanai Y. Genome-wide DNA methylation profiles in both precancerous conditions and clear cell renal cell carcinomas are correlated with malignant potential and patient outcome. *Carcinogenesis* 2009;30:214–21.
 27. Kanai Y, Ushijima S, Tsuda H, Sakamoto M, Hirohashi S. Aberrant DNA methylation precedes loss of heterozygosity on chromosome 16 in chronic hepatitis and liver cirrhosis. *Cancer Lett* 2000;148:73–80.
 28. Kondo Y, Kanai Y, Sakamoto M, Mizokami M, Ueda R, Hirohashi S. Genetic instability and aberrant DNA methylation in chronic hepatitis and cirrhosis—A comprehensive study of loss of heterozygosity and microsatellite instability at 39 loci and DNA hypermethylation on 8 CpG islands in microdissected specimens from patients with hepatocellular carcinoma. *Hepatology* 2000;32:970–9.
 29. Kanai Y, Saito Y, Ushijima S, Hirohashi S. Alterations in gene expression associated with the overexpression of a splice variant of DNA methyltransferase 3b, DNMT3b4, during human hepatocarcinogenesis. *J Cancer Res Clin Oncol* 2004;130:636–44.
 30. Chang MH, Chen CJ, Lai MS, Hsu HM, Wu TC, Kong MS, Liang DC, Shau WY, Chen DS. Universal hepatitis B vaccination in Taiwan and the incidence of hepatocellular carcinoma in children. Taiwan Childhood Hepatoma Study Group. *N Engl J Med* 1997;336:1855–9.
 31. Tanaka Y, Hanada K, Mizokami M, Yeo AE, Shih JW, Gojbori T, Alter HJ. Inaugural article: a comparison of the molecular clock of hepatitis C virus in the United States and Japan predicts that hepatocellular carcinoma incidence in the United States will increase over the next two decades. *Proc Natl Acad Sci USA* 2002;99:15584–9.
 32. Park IY, Sohn BH, Yu E, Suh DJ, Chung YH, Lee JH, Surzycki SJ, Lee YI. Aberrant epigenetic modifications in hepatocarcinogenesis induced by hepatitis B virus X protein. *Gastroenterology* 2007; 132:1476–94.
 33. Arase Y, Ikeda K, Suzuki F, Suzuki Y, Kobayashi M, Akuta N, Hosaka T, Sezaki H, Yatsuji H, Kawamura Y, Kobayashi M, Kumada H. Comparison of interferon and lamivudine treatment in Japanese patients with HBeAg positive chronic hepatitis B. *J Med Virol* 2007; 79:1286–92.
 34. Yoshida H, Tateishi R, Arakawa Y, Sata M, Fujiyama S, Nishiguchi S, Ishibashi H, Yamada G, Yokosuka O, Shiratori Y, Omata M. Benefit of interferon therapy in hepatocellular carcinoma prevention for individual patients with chronic hepatitis C. *Gut* 2004;53:425–30.
 35. Oikawa T, Ojima H, Yamasaki S, Takayama T, Hirohashi S, Sakamoto M. Multistep and multicentric development of hepatocellular carcinoma: histological analysis of 980 resected nodules. *J Hepatol* 2005;42:225–9.



For reprint orders, please contact: reprints@futuremedicine.com

DNA methylation profiles in precancerous tissue and cancers: carcinogenetic risk estimation and prognostication based on DNA methylation status

Alterations in DNA methylation, which are associated with DNA methyltransferase abnormalities and result in silencing of tumor-related genes and chromosomal instability, are involved even in precancerous changes in various organs. DNA methylation alterations also account for the histological heterogeneity and clinicopathological diversity of human cancers. Therefore, we have analyzed DNA methylation on a genome-wide scale in clinical tissue samples. Our approach using the bacterial artificial chromosome array-based methylated CpG island amplification method has revealed that DNA methylation alterations correlated with the future development of more malignant cancers are already accumulated at the precancerous stage in the kidney, liver and urinary tract. DNA methylation profiles at precancerous stages are basically inherited by the corresponding cancers developing in individual patients. Such DNA methylation alterations may confer vulnerability to further genetic and epigenetic alterations, generate more malignant cancers, and thus determine patient outcome. On the basis of bacterial artificial chromosome array-based methylated CpG island amplification data, indicators for carcinogenetic risk estimation have been established using liver tissue specimens from patients with hepatitis virus infection, chronic hepatitis and liver cirrhosis or histologically normal urothelia, and for prognostication using biopsy or surgically resected specimens from patients with renal cell carcinoma, hepatocellular carcinoma and urothelial carcinoma. Such genome-wide DNA methylation profiling has now firmly established the clinical relevance of translational epigenetics.

KEYWORDS: bacterial artificial chromosome array-based methylated CpG island amplification DNA methylation DNA methyltransferase precancerous condition prognostication risk estimation

Eri Arai¹ & Yae Kanai^{1*}

¹Pathology Division, National Cancer Center Research Institute, 5-1-1 Tsukiji, Chuo-ku, Tokyo 104-0045, Japan

*Author for correspondence:

Tel.: +81 335 422 511

Fax: +81 332 482 463

ykanai@ncc.go.jp

DNA methylation, a covalent chemical modification resulting in the addition of a methyl group at the carbon 5 position of the cytosine ring in CpG dinucleotides, is one of the most consistent epigenetic changes occurring in human cancers [1–3]. DNA methylation normally promotes a highly condensed heterochromatin structure associated with deacetylation of histones H3 and H4, loss of histone H3 lysine 4 (H3K4) methylation, and gain of H3K9 and H3K27 methylation [4–6]. DNA methylation is a stable modification inherited throughout successive cell divisions, and is essential for X-chromosome inactivation, genome imprinting, silencing of transposons and other parasitic elements, and proper expression of genes [7].

Human cancer cells show a drastic change in DNA methylation status, specificity in the overall DNA hypomethylation and regional DNA hypermethylation [1–3]. In 1995, when the *RB* and *VHL* genes were the only tumor suppressor genes known to be silenced by DNA methylation, we showed for the first time that the E-cadherin tumor suppressor gene is silenced by DNA methylation around the promoter region [8], and

proposed the universality of a ‘two-hit’ mechanism involving DNA hypermethylation and loss of heterozygosity during carcinogenesis. The list of tumor-related genes whose levels of expression are altered owing to DNA hypo- or hypermethylation has been increasing [9]. At this point, some explanation is necessary regarding the mechanisms whereby tumor-related genes whose DNA methylation status is altered during carcinogenesis are selected. One, but likely not the only, explanation for such selection is polycomb binding, in which CpG-rich sequences targeted by the polycomb complex in normal embryonic stem cells consequently form a bivalent domain carrying both ‘activating’ H3K4 methylation and ‘inactivating’ H3K27 methylation [10]. This bivalent state is converted to a primary active or repressive chromatin conformation after differentiation cues have been received. During carcinogenesis, such modifications may render the genes vulnerable to errors, resulting in aberrant DNA methylation [11].

On the other hand, DNA hypomethylation induces chromosomal instability through decondensation of heterochromatin and enhancement

future
medicine part of fsg

of chromosomal recombination during carcinogenesis [12]. For example, in hepatocellular carcinoma (HCC) [13] and urothelial carcinoma (UC) [14], DNA hypomethylation of pericentromeric satellite regions is correlated with copy number alterations on chromosomes 1 and 9, where such regions are found abundantly. A DNA methyltransferase (DNMT), DNMT3b, is required for DNA methylation of pericentromeric satellite regions in early mouse embryos [15]. We have demonstrated the possibility that an inactive splice variant, DNMT3b4 is upregulated, competes with DNMT3b3, the major splice variant in normal liver tissue, for targeting to pericentromeric satellite regions, and may lead to chromosomal instability through induction of DNA hypomethylation in such regions during hepatocarcinogenesis [16].

Translational epigenetics has now come of age [17–19], and the empirical analysis of DNA methylation status in clinical tissue samples with reference to the clinicopathological parameters of human cancers is becoming increasingly important for the diagnosis, prevention and therapy of cancers [20–22].

DNA methylation alterations during multistage carcinogenesis

Accumulating evidence suggests that alterations of DNA methylation may play a significant role even at precancerous stages in association with chronic inflammation, persistent infection with viruses and other pathogenic microorganisms, such as hepatitis B virus (HBV) or hepatitis C virus (HCV) [23–25], Epstein–Barr virus [26], human papillomavirus [27], and *Helicobacter pylori* [28] and cigarette smoking [29]. In the 1990s, we frequently observed DNA hypermethylation on C-type CpG islands, which are generally methylated in a cancer-specific but not age-dependent manner [30], and DNA methylation alterations at ‘hot spots’ of loss of heterozygosity in HCCs, even in samples of noncancerous liver tissue showing chronic hepatitis or liver cirrhosis, which are widely considered to be precancerous conditions, in comparison with normal liver tissue samples [23–25]. These findings [23] represented some of the earliest reports of DNA methylation alterations at the precancerous stage. Silencing of the E-cadherin gene, which encodes a Ca²⁺-dependent cell–cell adhesion molecule, in samples of noncancerous liver tissue showing chronic hepatitis or cirrhosis may result in heterogeneous E-cadherin expression, which is associated with small focal areas where hepatocytes show only slight

E-cadherin immunoreactivity [31]. Silencing of the E-cadherin gene may participate even in the very early stage of hepatocarcinogenesis through loss of intercellular adhesiveness and destruction of tissue morphology. Expression levels of mRNA for DNMT1, the major and best known DNMT, are significantly higher in 48 samples of noncancerous liver tissue showing chronic hepatitis or cirrhosis than in normal liver tissue, and are even higher in 67 samples of HCCs [32]. The incidence of DNMT1 overexpression in 53 samples of HCCs is significantly correlated with poorer tumor differentiation and portal vein involvement [33]. Moreover, the recurrence-free and overall survival rates of patients with HCCs showing DNMT1 overexpression are significantly lower than those of patients with HCCs that do not [33].

Ductal carcinomas of the pancreas frequently develop after chronic damage owing to pancreatitis. At least a proportion of peripheral pancreatic ductal epithelia with an inflammatory background may be at precancerous stages. We conducted an immunohistochemical analysis of DNMT1 in 48 samples of peripheral pancreatic duct epithelia showing no remarkable histological findings without an inflammatory background, 54 samples of peripheral pancreatic duct epithelia with an inflammatory background, 188 samples of another precancerous lesion, pancreatic intraepithelial neoplasia (PanIN), and 220 areas of invasive ductal carcinoma from surgical specimens resected from 100 patients (5, 24, 49 and 22 patients at Stage I to II, III, IVa and IVb, respectively) [34]. DNA methylation status of the *p14*, *p15*, *p16*, *p73*, *APC*, *hMLH1*, *MGMT*, *BRCA1*, *GSTP1*, *TIMP-3*, *CDH1* and *DAPK-1* genes was also analyzed in tissue samples during pancreatic carcinogenesis. To examine DNA methylation status in tiny tissue samples of peripheral pancreatic duct epithelia without or with an inflammatory background, avoiding any contamination with surrounding acinar cells and/or lymphocytes, we employed a method combining tissue microdissection with agarose bead-based bisulfite conversion followed by nested methylation-specific PCR: preheated low-melting agarose was mixed with the harvested microdissected tissue samples and the mixtures were pipetted into chilled mineral oil to form agarose beads. The beads with the tissue were incubated with proteinase K followed by bisulfite conversion. After neutralization with hydrochloric acid, the beads were used directly for nested methylation-specific PCR. This method also allowed us to examine the DNA methylation

status in PanIN and ductal carcinoma, avoiding contamination by the abundant desmoplastic stroma. The incidence of DNMT1 protein expression [34] and the average number of methylated tumor-related genes [35] increased with progression from peripheral pancreatic ductal epithelia with an inflammatory background, to PanIN, to well differentiated ductal carcinoma, and finally, to a poorly differentiated ductal carcinoma, in comparison with normal peripheral pancreatic duct epithelia without an inflammatory background. DNMT1 overexpression in ductal carcinomas of the pancreas is significantly correlated with the extent of invasion to the surrounding tissue, an advanced stage, poorer patient outcome [34], and accumulation of DNA methylation of tumor-related genes [35]. Although the maintenance activities of DNMT1 are related to its *in vitro* preference for hemimethylated substrates [36], excessive amounts of DNMT1 in comparison to those of proliferating cell nuclear antigen, which targets DNMT1 to replication foci [37], may participate in *de novo* methylation of CpG islands [38]. In fact, significant correlation between DNMT1 overexpression and accumulation of DNA methylation of specific genes in cell lines, mouse models and clinical tissue samples of various cancers has also been reported by other groups [39–43]. However, other groups have stated that they did not find such significant correlations [44–46]. Therefore, the participation of DNMT1 overexpression in accumulation of DNA methylation of tumor-related genes remains a controversial issue.

Genome-wide DNA methylation analysis

Recently, it has become possible to analyze DNA methylation on a genome-wide scale. The fact that DNA methylation alterations are associated with multistage carcinogenesis has prompted us to perform such genome-wide analysis in tissue specimens. The methods most commonly used to read methylated cytosines are a DNA methylation-sensitive restriction enzyme-based approach, such as the well-established technique of methylated CpG island amplification [47], affinity-based approaches, whereby antimethylcytosine antibody or methyl-binding domain proteins are used to enrich methylated fractions of genomic DNA, and bisulfite conversion of non-methylated cytosines to thymidine through hydrolytic deamination. These strategies for revealing methylated cytosines have been applied mainly to array platforms [48], and the resolution of the microarrays has been markedly

improved [49,50]. In addition to the introduction of new-generation sequencing technologies for bisulfite-converted genomic sequencing [48], a high-throughput technique without bisulfite conversion has been developed based on single-molecule, real-time DNA sequencing [51]. These new technologies will be able to efficiently reveal genome-wide DNA methylation profiles in tissue samples.

At the present time, many researchers in the field of cancer epigenetics use mainly promoter arrays to identify the genes that are silenced by DNA methylation in cancer cells. However, the promoter regions of specific genes are not the only target of DNA methylation alterations in human cancers. DNA methylation status in genomic regions that do not directly participate in gene silencing, such as the edges of CpG islands, may be altered at precancerous stages before the alterations of the promoter regions themselves occur [52]. Genomic regions in which DNA hypomethylation affects chromosomal instability may not be contained in promoter arrays. Moreover, aberrant DNA methylation of large regions of chromosomes, which are regulated in a coordinated manner in human cancers owing to a process of long-range epigenetic silencing, has recently attracted attention [53]. Therefore, we have recently employed bacterial artificial chromosome (BAC) array-based methylated CpG island amplification (BAMCA; FIGURE 1) [54]. Test or reference DNA was first digested with the methylation-sensitive restriction enzyme *Sma*I and subsequently with the methylation-insensitive *Xma*I. Adapters were ligated to the *Xma*I-digested sticky ends, and PCR was performed with an adapter primer set. Test and reference PCR products were labeled by random priming with Cy3- and Cy5-dCTP, respectively, and precipitated together with ethanol in the presence of Cot-I DNA. The mixture was applied to a custom-made array harboring approximately 4500 BAC clones located throughout chromosomes 1 to 22, X and Y.

Even though the resolution of BAMCA is inferior to the abovementioned newly developed high-resolution arrays, BAMCA has an ability for detecting any tendency for coordinated regulation of DNA methylation at multiple CpG sites in individual large regions of chromosomes, because any region covered by one BAC contains multiple *Sma*I sites. In fact, we validated this ability by the quantitative evaluation of DNA methylation status at each *Sma*I site on representative BAC clones by pyrosequencing: when almost all *Sma*I sites on

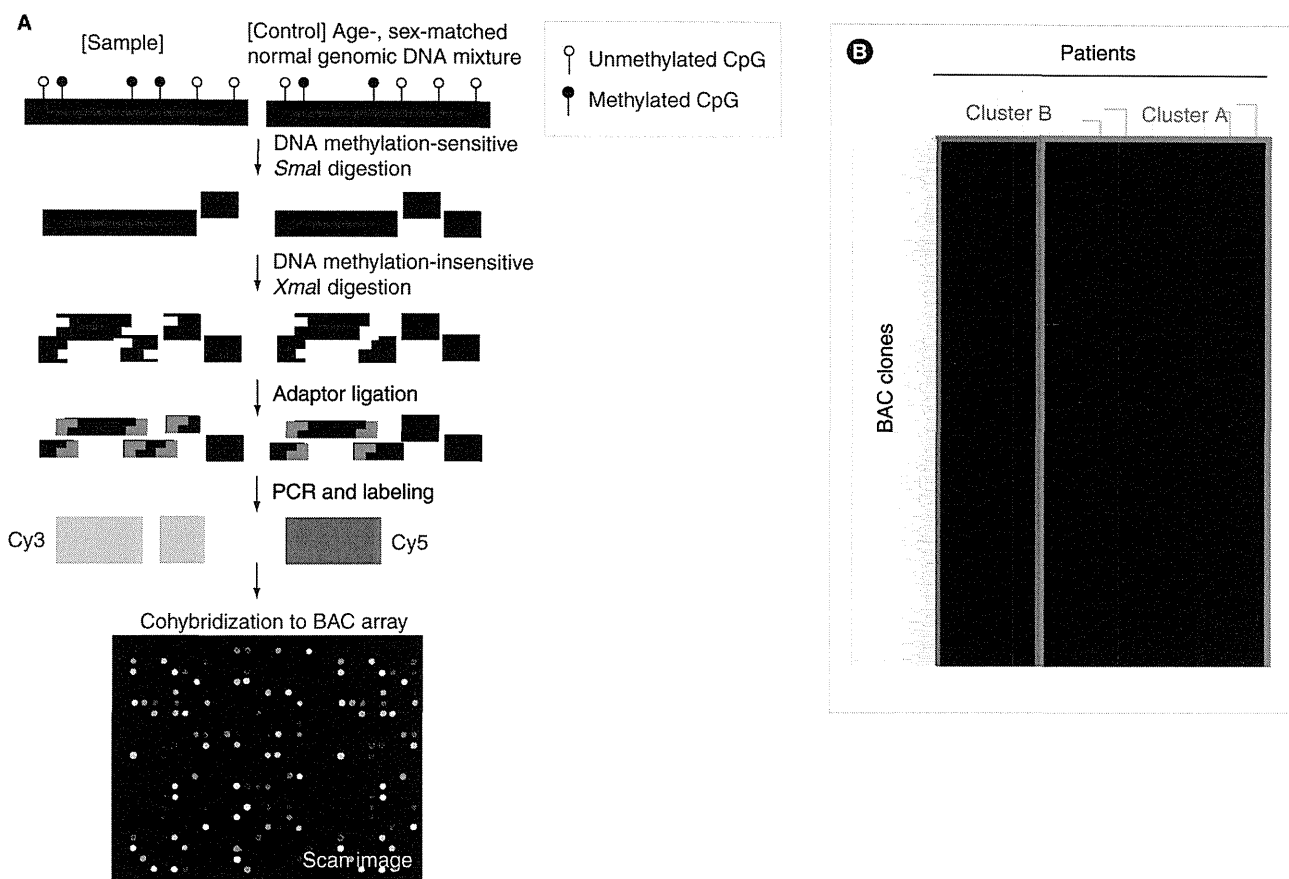


Figure 1. Bacterial artificial chromosome array-based methylated CpG island amplification in tissue samples.

(A) BAC array-based methylated CpG island amplification (BAMCA) method and an example of a scan image. **(B)** An example of unsupervised 2D hierarchical clustering analysis of patients with cancers based on BAMCA data. Patients with cancers are frequently clustered into subclasses associated with distinct DNA methylation profiles and distinct clinicopathological parameters. BAC: Bacterial artificial chromosome.

a BAC clone simultaneously showed lower or higher DNA methylation rates in comparison with those of normal tissues by pyrosequencing, the signal ratio on the BAC clone demonstrated by BAMCA showed DNA hypo- or hyper-methylation, respectively [55]. BAMCA has also been used by other groups to identify tumor-related genes whose expression levels are regulated by DNA methylation in human cancer cells [56–58].

Genome-wide DNA methylation profiles in precancerous stages are inherited by cancers & determine the tumor aggressiveness

With respect to renal cell carcinomas (RCCs), DNA methylation profiling of more than 800 genes has been reported in both Von Hippel Lindau-related and -unrelated RCCs, and it is known that genes linked to TGF- β or ERK/Akt signaling are preferentially methylated in papillary RCCs in comparison to clear cell RCCs [59]. However, precancerous

conditions in the kidney have rarely been described because of the lack of any remarkable histological changes, or association with chronic inflammation and persistent infection with viruses or other pathogenic microorganisms. The DNA methylation status of noncancerous renal tissues obtained from patients with RCCs has not been analyzed in detail. When BAMCA methods were applied to 51 samples of noncancerous renal tissue obtained from patients with clear cell RCCs, many BAC clones showed DNA hypo- or hyper-methylation in comparison to normal renal tissue samples from patients without any primary renal tumors [60]. From the viewpoint of DNA methylation, we can consider that noncancerous renal tissue from patients with RCCs is already at precancerous stages, showing genome-wide DNA methylation alterations [60].

We then performed unsupervised 2D hierarchical clustering analysis based on BAMCA data for noncancerous renal tissue samples. The

patients with RCCs were clustered into two subclasses, clusters A_{NK} and B_{NK} [60]. Tumors developing in individual patients belonging to cluster B_{NK} were clinicopathologically more aggressive than those in cluster A_{NK} . The overall survival rate of patients in cluster B_{NK} was significantly lower than that of patients in cluster A_{NK} . Aggressiveness of the corresponding tumors and even patient outcome may thus be determined by DNA methylation profiles at precancerous stages.

Renal cell carcinomas are usually well demarcated, being surrounded by a fibrous capsule, and hardly ever contain a fibrous stroma. Therefore, we were able to obtain cancer cells of high purity from fresh surgical specimens, avoiding contamination with both noncancerous epithelial cells and stromal cells. When we analyzed 51 samples of RCC (30, 16 and 5 patients at Stage I to II, III and IV, respectively), more BAC clones showed DNA hypo- or hyper-methylation, and its degree was increased in comparison with samples of noncancerous renal tissue obtained from patients with RCCs. Unsupervised 2D hierarchical clustering analysis based on BAMCA data for RCCs was able to group patients into two subclasses, clusters A_{TK} and B_{TK} [60]. Clinicopathologically aggressive tumors were accumulated in cluster B_{TK} . The overall survival rate of patients in cluster B_{TK} was significantly lower than that of patients in cluster A_{TK} .

All patients who were grouped in cluster B_{NK} on the basis of BAMCA data for noncancerous renal tissue were included in cluster B_{TK} on the basis of BAMCA data for the RCCs themselves [60]. The majority of the BAC clones significantly discriminating cluster B_{NK} from cluster A_{NK} also discriminated cluster B_{TK} from cluster A_{TK} . Among BAC clones characterizing both clusters B_{NK} and B_{TK} , where the average signal ratio of cluster B_{NK} was higher than that of cluster A_{NK} , the average signal ratio of cluster B_{TK} was also higher than that of cluster A_{TK} without exception (FIGURE 2A). Among BAC clones characterizing both clusters B_{NK} and B_{TK} , where the average signal ratio of cluster B_{NK} was lower than that of cluster A_{NK} , the average signal ratio of cluster B_{TK} was also lower than that of cluster A_{TK} without exception (FIGURE 2A). Comparison between the signal ratios of each BAC clone characterizing both clusters B_{NK} and B_{TK} revealed that the DNA methylation status of the noncancerous renal tissue was basically inherited by the corresponding RCC in each individual patient (FIGURE 2B) [60].

In noncancerous renal tissue showing no remarkable histological changes and consisting mainly of renal tubules with specialized functions, no progenitor cell is able to gain a growth advantage, and clonal expansion is unable to occur. Therefore, the distinct DNA methylation profiles of cluster B_{NK} cannot be established through the selection of one of a number of random DNA methylation profiles in noncancerous renal tissue, and instead may be established through distinct target mechanisms. Since the DNA methylation profiles in cluster B_{TK} are shared by phenotypically similar patients, who all suffer from clinicopathologically aggressive tumors and show a poor outcome, DNA methylation alterations in at least a proportion of the BAC regions characterizing cluster B_{TK} cannot be passenger changes. DNA methylation alterations of BAC regions characterizing cluster B_{TK} may significantly participate in carcinogenesis, since the DNA methylation profiles in cluster B_{NK} were established at very early stages of carcinogenesis and inherited during progression of the cancers themselves as cluster B_{TK} . At least a proportion of DNA methylation alterations at precancerous stages may be 'epigenetic gatekeepers' [2], which allow time for further epigenetic and genetic alterations.

In fact, when the DNA methylation status on CpG islands of the *p16*, *hMLH1*, *VHL* and *THBS-1* genes, and the methylated in tumor (MINT)-1, -2, -12, -25 and -31 clones were examined by bisulfite modification in the same cohort, genome-wide DNA methylation alterations consisting of both hypo- and hyper-methylation revealed by BAMCA in cluster B_{TK} were frequently associated with accumulation of regional DNA hypermethylation on these CpG islands [61]. For comparison with BAMCA data, we also examined copy number alterations by array-based comparative genomic hybridization using the same BAC array in the same cohort. By unsupervised hierarchical clustering analysis based on copy number alterations, RCCs were clustered into the two subclasses, clusters GA_{TK} and GB_{TK} [62]. Copy number alterations were accumulated in the cluster GB_{TK} . Loss of chromosome 3p and gain of 5q and 7 were frequent in both clusters GA_{TK} and GB_{TK} , whereas loss of 1p, 4, 9, 13q and 14q was frequent only in cluster GB_{TK} [62]. Clear cell RCCs showing higher histological grades, vascular involvement, renal vein tumor thrombi and higher pathological stages were accumulated in cluster GB_{TK} [62]. The recurrence-free and overall survival rates of patients in cluster GB_{TK} were

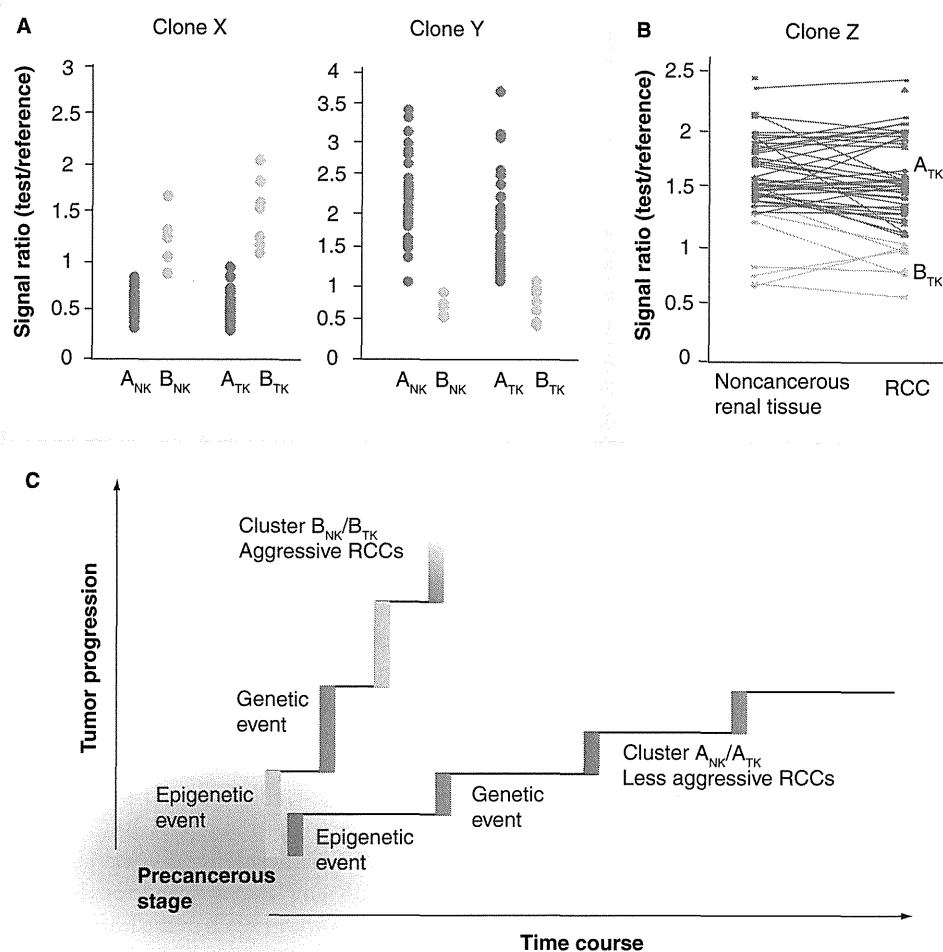


Figure 2. DNA methylation profiles in precancerous conditions and renal cell carcinomas.

(A) Correlation between DNA methylation profiles of precancerous conditions and those of RCCs. Cluster B_{NK} was completely included in cluster B_{TK} . The majority of the bacterial artificial chromosome (BAC) clones, 724 in all, significantly discriminating cluster B_{NK} from cluster A_{NK} , also discriminated cluster B_{TK} from cluster A_{TK} . In 311 of the 724 BAC clones, where the average signal ratio of cluster B_{NK} was higher than that of cluster A_{NK} , such as clone X, the average signal ratio of cluster B_{TK} was also higher than that of cluster A_{TK} without exception. In 413 of the 724 BAC clones, where the average signal ratio of cluster B_{NK} was lower than that of cluster A_{NK} , such as clone Y, the average signal ratio of cluster B_{TK} was also lower than that of cluster A_{TK} without exception. **(B)** Scattergram of the signal ratios in samples of noncancerous renal tissue and RCCs for all patients examined for a representative BAC clone, clone Z. The DNA methylation status of the noncancerous renal tissue was basically inherited by the corresponding RCC in individual patients. **(C)** Significance of DNA methylation alterations at precancerous stages. Regional DNA hypermethylation of C-type CpG islands and copy number alterations were accumulated in cluster B_{TK} . In other words, DNA methylation alterations in precancerous conditions, such as DNA methylation profiles corresponding to cluster B_{NK} , may not occur randomly but may be prone to further accumulation of epigenetic and genetic alterations, thus generating more malignant cancers, such as the RCCs in patients belonging to cluster B_{TK} . RCC: Renal cell carcinoma.

significantly lower than those of patients in cluster GA_{TK} [62]. Multivariate analysis revealed that genetic clustering was a predictor of recurrence-free survival, and was independent of histological grade and pathological stage [62]. A subclass of cluster B_{TK} based on BAMCA data was completely included in cluster GB_{TK}

showing accumulation of copy number alterations. Genetic and epigenetic alterations are not mutually exclusive during renal carcinogenesis, and particular DNA methylation profiles may be closely related to chromosomal instability. DNA methylation alterations at precancerous stages, which may not occur randomly but may

foster further epigenetic and genetic alterations, can generate more malignant cancers and even determine patient outcome (FIGURE 2C).

Even though high-throughput detection technologies have recently been developed, the dynamics of DNA methylation at repetitive sequences and gene bodies still remain to be determined [7]. However, our BAC array-based methods do not focus only on specific promoter regions and CpG islands, and have successfully identified the BAC regions including non-unique sequences in which coordinated DNA methylation alterations have clinicopathological impact. Evaluation of the correlation between the DNA methylation status of identified repetitive sequences and gene bodies, and the clinicopathological diversity of cancers may provide new insights into the roles of DNA methylation during multistage carcinogenesis.

Carcinogenetic risk estimation based on DNA methylation profiles

With respect to HCCs, the results of analysis of DNA methylation status of CpG islands of multiple genes have been reported. Some groups have attempted to use DNA methylation profiles as molecular markers of early HCCs or as prognostic indicators for patients with HCCs [63,64]. Since BAMCA detects DNA methylation alterations that are regulated in a coordinated manner at multiple CpG sites in individual large regions of chromosomes, BAMCA may be able to identify unique diagnostic indicators that may be overlooked by other technologies. We then applied the BAMCA method to multistage hepatocarcinogenesis. HCCs are known to be medullary tumors without a fibrous stroma. Therefore, we were able to obtain cancer cells of high purity from fresh surgical specimens, avoiding any contamination with stromal cells. In samples of noncancerous liver tissue obtained from patients with HCCs, many BAC clones showed DNA hypo- or hyper-methylation in comparison with normal liver tissue from patients without HCCs. Patients showing DNA hypo- or hyper-methylation on more BAC clones in their samples of noncancerous liver tissue frequently developed metachronous or recurrent HCCs after hepatectomy [65], suggesting that DNA methylation alterations at precancerous stages may not occur randomly but tend to lead to the development of more malignant HCCs.

The effectiveness of surgical resection for HCC is limited, unless the disease is diagnosed early at the asymptomatic stage. Therefore, surveillance at precancerous stages is a priority. To

reveal the baseline liver histology, microscopy examination of liver biopsy specimens is performed for patients with hepatitis virus infection prior to interferon therapy. Therefore, carcinogenetic risk estimation using such liver biopsy specimens would be advantageous for close follow-up of patients who are at high risk of HCC development.

Inflammation itself can induce drastic DNA methylation alterations at the chronic hepatitis stage. Although a proportion of such alterations do participate in progression to HCC, the remaining inflammation-associated DNA methylation alterations may diminish after the hepatitis stage has passed and as HCC develops. DNA methylation alterations associated only with inflammation and not with carcinogenesis cannot be regarded as indicators for carcinogenetic risk estimation in patients who are being followed up owing to chronic hepatitis. Therefore, to estimate the degree of carcinogenetic risk based on DNA methylation profiles, we focused on BAC clones for which DNA methylation status was altered at the chronic hepatitis and liver cirrhosis stages and were inherited by HCCs from such precancerous stages. Among them, a bioinformatics approach identified the top 25 BAC clones for which DNA methylation status was able to discriminate 15 samples of noncancerous liver tissue from patients with HCCs in the learning cohort from 10 samples of normal liver tissue with sufficient sensitivity and specificity. We established the criteria for carcinogenetic risk estimation by combining the cutoff values of signal ratios for the 25 BAC clones (FIGURE 3A). Based on these criteria, the sensitivity and specificity for diagnosis of noncancerous liver tissue samples obtained from patients with HCCs in the learning cohort as being at high risk of carcinogenesis were both 100% [65]. Our criteria enabled diagnosis of additional noncancerous liver tissue samples obtained from patients with HCCs in the validation cohort ($n = 50$) as being at high risk of carcinogenesis with a sensitivity and specificity of 96% [65].

The number of BAC clones satisfying the criteria in noncancerous liver tissue samples showing chronic hepatitis obtained from patients with HCCs was not significantly different from that in noncancerous liver tissue samples showing cirrhosis obtained from patients with HCCs. In addition, the average number of BAC clones satisfying the criteria was significantly lower in samples of liver tissue obtained from patients who were infected with HBV or HCV, but who had never developed HCCs, than that in noncancerous liver tissue samples obtained from

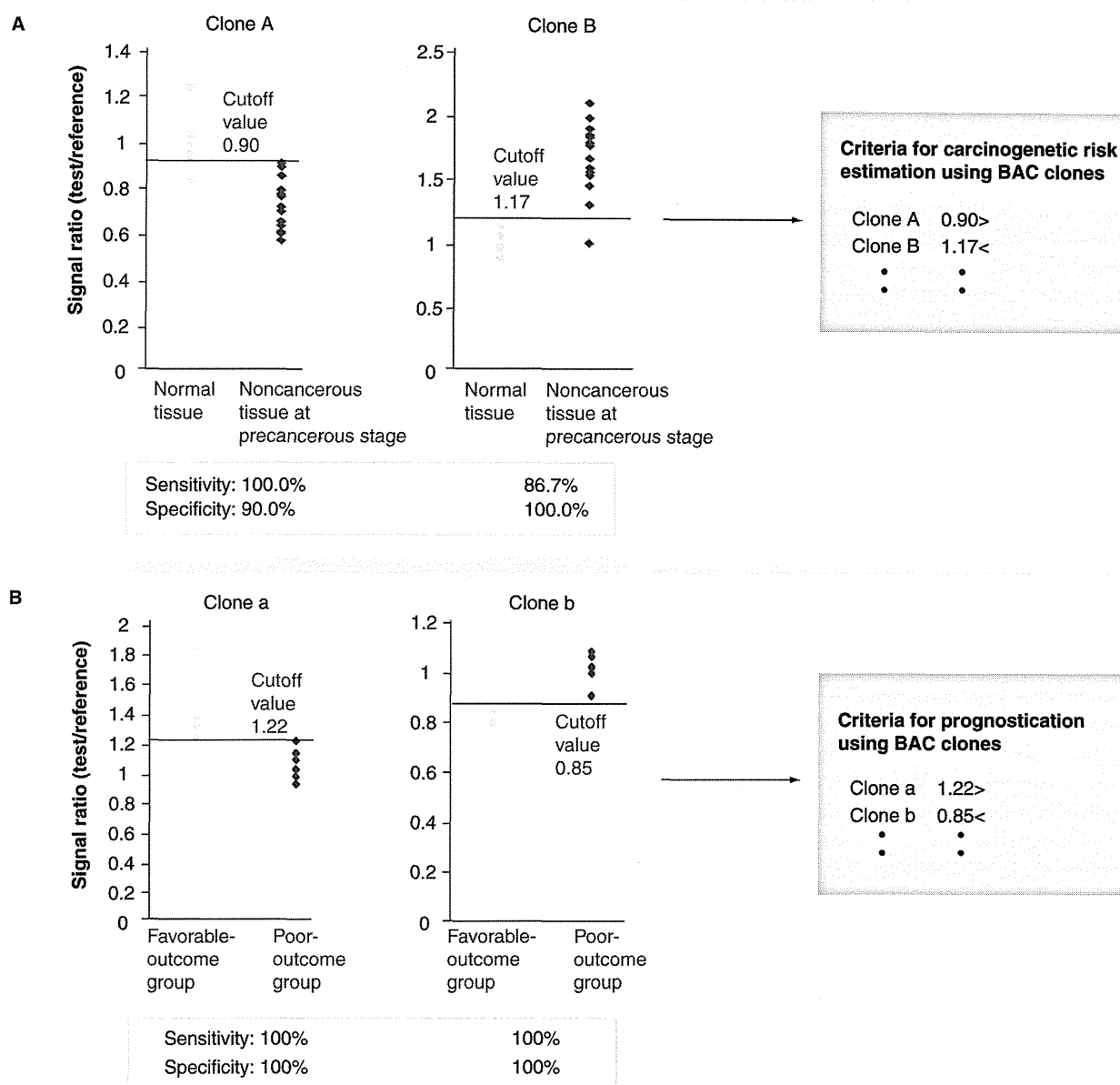


Figure 3. Carcinogenetic risk estimation and prognostication of patients with cancers based on DNA methylation status.

(A) Carcinogenetic risk estimation based on DNA methylation status. Examples of scattergrams of the signal ratios in normal tissue samples and noncancerous tissue samples at precancerous stages for representative BAC clones, clone A and clone B. Using the cutoff values in each panel, noncancerous tissue samples at precancerous stages were discriminated from normal tissue samples with sufficient sensitivity and specificity. Based on a combination of the cutoff values for the selected BAC clones, the criteria for carcinogenetic risk estimation were established. **(B)** Prognostication of patients with cancers based on DNA methylation status. Examples of scattergrams of the signal ratios in the favorable-outcome group and poor-outcome group for representative BAC clones, clone a and clone b. Using the cutoff values in each panel, patients belonging to the poor-outcome group were discriminated from those belonging to the favorable-outcome group. Based on a combination of the cutoff values for the selected BAC clones, the criteria for prognostication were established.

BAC: Bacterial artificial chromosome.

patients with HCCs. Therefore, our criteria may be applicable for classifying liver tissue obtained from patients who are followed up because of hepatitis virus infection, chronic hepatitis or liver cirrhosis into that which may generate HCCs and that which will not [65].

Next, we quantitatively examined the DNA methylation status at each *XmaI/SmaI* site on the 25 BAC clones by pyrosequencing. The sensitivity and specificity of the criteria revised by pyrosequencing have been successfully improved by using CpG sites having the largest diagnostic